

Protein visualization and manipulation in *Drosophila* through the use of epitope tags recognized by nanobodies

Jun Xu^{1, #, *}, Ah-Ram Kim^{1, #}, Ross W. Cheloha², Fabian A. Fischer², Joshua Shing Shun Li¹, Yuan Feng¹, Emily Stoneburner¹, Richard Binari¹, Stephanie E. Mohr^{1, 3}, Jonathan Zirin^{1, 3}, Hidde Ploegh² and Norbert Perrimon^{1, 3, 4, 5, *}

¹ Department of Genetics, Blavatnik Institute, Harvard Medical School, Boston, Massachusetts, USA.

² Boston Children's Hospital and Harvard Medical School, Boston, Massachusetts, USA.

³ Drosophila RNAi Screening Center, Harvard Medical School, Boston, Massachusetts, USA.

⁴ Howard Hughes Medical Institute, Boston, Massachusetts, USA.

⁵ Lead Contact

co-first authors

*Correspondence: Jun_Xu@hms.harvard.edu; perrimon@genetics.med.harvard.edu.

SUMMARY

Expansion of the available repertoire of reagents for visualization and manipulation of proteins will help understand their function. Short epitope tags installed on proteins of interest and recognized by existing binders such as nanobodies facilitate protein studies by obviating the need to isolate new antibodies directed against them. Nanobodies have several advantages over conventional antibodies, as they can be expressed and used as tools for visualization and manipulation of proteins *in vivo*. Here, we combine the advantages of short epitopes (NanoTags) and nanobodies specific for them by characterizing two short (<15 aa) tags, 127D01 and VHH05, which are high-affinity targets of nanobodies. We demonstrate that these NanoTags and the nanobodies that recognize them can be used in *Drosophila* for *in vivo* protein detection and re-localization, direct and indirect immunofluorescence, immunoblotting, and immunoprecipitation. We further show that CRISPR-mediated gene targeting provides a straightforward approach to tagging endogenous proteins with the NanoTags. Single copies of the NanoTags, regardless of their location, suffice for detection. This versatile and validated toolbox of tags and nanobodies will serve as a resource for a wide array of applications, including functional studies in *Drosophila* and beyond.

INTRODUCTION

Conventional antibodies typically have a MW ~150-160 kDa and are composed of four polypeptides, two identical heavy chains and two identical light chains. Size and composition of conventional immunoglobulins impose limitations on their application to *in vivo* studies. The recent development of smaller and single-polypeptide recombinant protein binders, such as single chain variable fragments (scFvs, ~25kDa), single-domain antibodies or 'nanobodies' (~12-15kDa), and designed ankyrin repeat proteins (DARPs, 18 kDa for five repeats), has enabled many new applications (Harmansa and Affolter, 2018). These new types of recombinant binders are small and stable molecules that can be encoded in the genomes of model organisms or cells. Moreover, the coding sequences of these binders can be fused to various effector domains, making them useful as tools for imaging and for regulating the function of target proteins of interest (POIs) *in vivo* (Helma et al., 2015; Harmansa and Affolter, 2018; Aguilar et al., 2019). For example, a protein binder fused to a fluorescent protein can be expressed *in vivo*, where it can then bind to an endogenous target protein, an epitope-tagged protein, or even a post-translational modification, thus allowing visualization of subcellular localization of the target (Harmansa and Affolter, 2018; Aguilar et al., 2019). This is not usually possible when using conventional antibodies, which fail to assemble in the reducing environment of the cytosol.

Among available protein binders, camelid-derived nanobodies are particularly useful, as they consist of a single monomeric variable antibody domain that is the product of selection *in vivo*. Nanobodies are no less specific than conventional antibodies. Given their small size, nanobodies are easy to express in *Escherichia coli*, either alone or fused to a fluorescent marker or enzyme. The small size of nanobodies also allows better super-resolution microscopy than antibody-based imaging (Fornasiero and Opazo 2015; Mikhaylova et al., 2015; Virant et al., 2018; Fang et al., 2018), and enables binding to epitopes not accessible to full-length conventional antibodies. Because nanobodies are usually stable in the reducing environment of intracellular space and are encoded as a single polypeptide, nanobodies or nanobody fusion proteins can be expressed in eukaryotes and used for a number of *in vivo* applications (Helma et al., 2015).

Nanobodies are powerful tools for manipulation of protein function and localization, as has been illustrated using nanobodies against GFP. For example, GFP-tagged proteins can be degraded using a GFP-targeting nanobody fused to an E3 ligase component, an approach that has been used for studies in *Drosophila melanogaster*, *Caenorhabditis elegans*, and *Danio rerio* (Caussin et al., 2011; Wang et al., 2017; Yamaguchi et al., 2019). GFP-tagged proteins can be re-localized using a GFP-targeting nanobody fused to sequences or domains that specify a particular subcellular localization (Harmansa et al., 2015; Harmansa et al., 2017). Many proteins in model organisms such as *Drosophila* have been tagged with GFP, suggesting general applicability of the approach. However, the fusion of a target protein with GFP is not necessarily compatible with all applications, a significant limitation of a GFP-targeted approach. GFP is a bulky (27 kDa) substituent that might

affect function or localization of the tagged protein. In addition, maturation of the GFP chromophore is slow, limiting its use for the imaging of nascent proteins.

An alternative approach would be to combine conventional epitope tags with the advantages of nanobody-based targeting. Because of their small size, epitope tags are less likely than GFP to interfere with the overall structure of the tagged protein. Several nanobodies that recognize small epitope tags have been isolated, including tags known as BC2-tag, EPEA-tag, MoonTag, and ALFA-tag (Traenkle et al., 2015; De Genst et al., 2010; Boersma et al., 2019; Tanenbaum et al., 2014; Götzke et al., 2019; Cheloha et al., 2020). Some of these have been used to visualize and manipulate tagged proteins by changing their abundance or localization using tag-targeting nanobodies in mammalian cells (Zhao et al., 2019; Vigano et al., 2021). The recently developed ALFA nanobody (NbALFA) recognizes a short peptide of 13 amino acids and provides a system useful for immunoblotting, protein purification, and imaging (fixed or live cells) (Götzke et al., 2019). To the best of our knowledge, epitope tag-specific nanobodies have yet to be applied for use *in vivo* in *Drosophila* or other multicellular organisms.

To expand the repertoire of nanobody-recognized tags (NanoTags) and corresponding nanobody tools, we characterized two NanoTags, VHH05- and 127D01-tags, and their corresponding nanobodies, NbVHH05 (Ling et al., 2019) and Nb127D01, for cellular and *in vivo* studies in *Drosophila*. Both nanobodies can be genetically encoded as fluorescent protein fusions (i.e., chromobodies, CBs) that enable detection of target proteins that carry NanoTags at N-terminal, internal or C-terminal sites. We show that these nanobodies are useful for multiplexed immunostaining, immunoblotting, and immunoprecipitation. We show that NanoTagged proteins can be manipulated by nanobodies fused to various subcellular localization signals. Moreover, in transgenic flies that overexpress NanoTagged proteins, we confirmed that the tagged proteins can be detected using GFP-tagged nanobodies expressed *in vivo* (i.e. with CBs) or by immunostaining. Finally, using CRISPR-based genome engineering, we generated flies with NanoTags inserted into endogenous genes. Our data show that VHH05- and 127D01-tags and their corresponding nanobodies can be used effectively for labeling and manipulating proteins. These will be powerful tools for functional studies in *Drosophila* and other organisms.

RESULTS

Characterization of VHH05 and 127D01 NanoTags

We selected two nanobody/NanoTag pairs to test in *Drosophila*, NbVHH05/VHH05-tag and Nb127D01/127D01-tag. NbVHH05 is a 111 amino acid (aa) nanobody that recognizes a 14 aa sequence (VHH05-tag, QADQEAKELARQIS) derived from the human E2 ubiquitin-conjugating enzyme UBC6e (Fig. 1A and 1B), and has a binding constant (K_d) for the VHH05-tag of ~0.15 nM (Ling et al., 2019). Nb127D01 is a 115 aa nanobody that binds to an extracellular portion of the human C-X-C chemokine receptor type 2 (CXCR2) (Bradley et al., 2015). As the extracellular region of CXCR2 is large, we reduced the epitope-binding region to a minimal

sequence of 10 aa (127D01-tag, SFEDFWKGED) (Fig. 1C and 1D, Fig. S1) to obtain a more versatile tag, and determined the K_d of Nb127D01 to this tag to be <50 nM (data not shown). Protein-protein BLAST searches with both NanoTags failed to identify fully homologous sequences in the *Drosophila* proteome, thus reducing the possibility of spurious cross-reactions with endogenous, untagged proteins.

To determine whether these NanoTags can be used for live imaging, we visualized both the NanoTags and their corresponding nanobodies concurrently. To do this, we constructed vectors that use the *Actin5c* promoter to ubiquitously express mCherry proteins equipped with the NanoTags and with different cell compartment localization sequences at the N-terminus: a cell membrane localization protein (murine CD8 gene, NM_009857.1), a mitochondrial outer membrane sequence (TM domain of *Homo sapiens* CDGSH iron sulfur domain 1, NM_018464.5), and a nuclear localization sequence (histone H2B gene, NM_001032214.2). We also constructed vectors that ubiquitously express GFP-tagged nanobodies (NbVHH05-GFP and Nb127D01-GFP) (Fig. S2A and S2B) under the control of the *Actin5c* promoter.

When expressed alone in *Drosophila* S2R+ cells, NanoTagged mCherry fusion proteins were observed in the expected subcellular compartments (Fig. S2D), indicating that the VHH05- and 127D01-tags do not affect protein localization. When either NbVHH05-GFP or Nb127D01-GFP was expressed in cells, we observed a GFP signal in the nucleus and the cytoplasm (Fig. S2C). Next, we co-transfected S2R+ cells with either mCherry-VHH05 fusion proteins and NbVHH05-GFP or mCherry-127D01 fusion proteins and Nb127D01-GFP. In all cases, the GFP and mCherry signals colocalized and with a distribution indistinguishable from that of mCherry fusions alone (Fig. S2E and S2F). We also tested whether mCherry-tagged nanobodies (NbVHH05-mCherry or Nb127D01-mCherry) colocalized with mitochondrial GFP tagged with the VHH05-tag or the 127D01-tag, respectively. As expected, we observed colocalization of NbVHH05-mCherry and mito-GFP-VHH05 when expression vectors for each were co-transfected in S2R+ cells (Fig. S2G). Similarly, Nb127D01-mCherry and mito-GFP-127D01 colocalized with mitochondria (Fig. S2H).

We next examined whether the position of the NanoTags affects recognition by the nanobodies. We generated H2B-mCherry, mito-mCherry, and CD8-mCherry with N-terminal, internal, or C-terminal NanoTags. When these vectors were co-transfected with NbVHH05-GFP or Nb127D01-GFP in S2R+ cells, GFP and mCherry co-localized with the expected cellular compartments (Fig. 1E-1J). Taken together, our data show that both NbVHH05 and Nb127D01 can be used as CBs to visualize and monitor NanoTagged proteins in their native surroundings.

Detecting NanoTagged proteins by immunofluorescence

In addition to establishing CB-based detection of NanoTagged proteins in cells, we also explored detection by immunofluorescence. Nanobodies can be detected by either direct or indirect immunofluorescence. Direct immunofluorescence involves the use of fluorophore-conjugated nanobodies to detect the target protein(s). Indirect

immunofluorescence involves recognition of the target by the nanobody, followed by detection of the nanobody by a secondary fluorophore-conjugated antibody.

For direct immunofluorescence, we chemically conjugated NbVHH05 and Nb127D01 with fluorophores (NbVHH05-555 and Nb127D01-647). Success of these conjugations was confirmed by detection of a fluorescent signal on an SDS-PAGE gel (Fig. S4). Immunostaining with these fluorophore-conjugated nanobodies directly revealed VHH05- and 127D01-tagged proteins in S2R+ cells (Fig. 2A and Fig. 2A', Fig. S3A2). Direct immunostaining with fluorophore-conjugated nanobodies thus provides a simple and efficient method of detection. The reactivity of neither VHH05 nor 127D01 was affected by direct chemical conjugation. In addition, we used a fluorescent NbVHH05-555 prepared by sortase labeling (Guimaraes *et al.*, 2013) (Fig. S3A3). These chemoenzymatic reactions proceed near-quantitatively and are absolutely site-specific. Unlike chemical modification, the sortase labeling procedure does not entail the risk of unwanted side reactions that might otherwise affect the physicochemical properties of the final product. Because each enzymatically modified nanobody carries a single substituent (fluorophore or biotin), quantitative comparisons are in principle possible, which would be more challenging when using direct chemical conjugation.

To test VHH05 and 127D01 in indirect immunofluorescence, we prepared bacterially purified NbVHH05 and Nb127D01, each fused with an ALFA-tag or HA-tag. We also prepared conditioned media that contained NbVHH05 or Nb127D01 tagged with the Fc portion of human IgG (hIgG) (Fig. S3B5, Fig. S4). Consistent with a previous report (Götzke *et al.*, 2019), NbVHH05-ALFA and Nb127D01-ALFA can be visualized using anti-ALFA nanobodies conjugated to fluorophores (Fig. 2B, Fig. S3B2). We could visualize NbVHH05-HA and Nb127D01-HA using fluorescently labeled anti-HA antibodies (Fig. S3B3). Likewise, we could visualize NbVHH05-hIgG and Nb127D01-hIgG using fluorescently labeled anti-human IgG antibodies (Fig. S3B5). Next, we determined whether ALFA-, HA-, or hIgG-tagged NbVHH05 and Nb127D01 could be used as the primary reagents for indirect immunostaining. We stained S2R+ cells transfected with mito-GFP-VHH05 or mito-GFP-127D01 vectors with the corresponding primary and secondary antibodies. In both cases, the GFP signal overlapped completely with the fluorescent signal from the secondary antibody (Fig. 2B' and Fig. S3B). NbVHH05 and Nb127D01 were obtained by immunization of an alpaca and llama, respectively (Ling *et al.*, 2019; Bradley *et al.*, 2015). We therefore examined whether they are both recognized by fluorophore-conjugated anti-alpaca IgG 647 which is reactive with llama-derived nanobodies (or the VHH domain of llama IgG) (Fig. 2C). The NanoTagged GFP and 647-fluorophore signals overlapped completely (Fig. 2C' and Fig. S3B1), indicating that commercially available secondary antibodies against llama are compatible with NbVHH05 and Nb127D01 immunostaining. In addition, we carried out indirect immunofluorescence using NbVHH05-biotin prepared by sortase labeling (Guimaraes *et al.*, 2013) and obtained similar results (Fig. S3B4).

The availability of two different NanoTag-nanobody pairs opens the possibility for co-staining or co-detection with CBs. To test this, we generated proteins tagged with

both NanoTags (VHH05- and 127D01-tags) and used NbVHH05 and Nb127D01 fused to HA-tag or ALFA-tag with corresponding secondary antibodies for detection. Importantly, these two tagging systems operate orthogonally, as no co-localization signal was observed in cells transfected with 127D01-GFP and with H2B-mCherry-VHH05 or mito-mCherry-VHH05 (VHH05-GFP with H2B-mCherry-127D01 or mito-mCherry-127D01) (Fig. S5A). To further test co-detection, we inserted VHH05 at the N-terminus of the transcription factor REPTOR and 127D01 at its C-terminus (VHH05-REPTOR-127D01). When S2R+ cells were transfected with VHH05-REPTOR-127D01, the NbVHH05-HA signal (488-fluorophore) and the Nb127D01-ALFA signal (647-fluorophore) completely overlapped (Fig. 2D, D'). Our data show that immunostaining using both of the NanoTag-nanobody pairs can be multiplexed.

Detection of NanoTagged proteins on immunoblots

Because the two nanobodies recognize small linear epitopes, we anticipated that these nanobodies might be useful for immunoblotting under denaturing conditions as already shown for VHH05 (Ling et al., 2015). We performed immunoblotting experiments with cell lysates containing VHH05- or 127D01-tagged H2B-mCherry. Using NbVHH05-ALFA and Nb127D01-ALFA as primary nanobodies, we detected a signal using NbALFA-HRP as the secondary antibody. Using purified nanobodies at high concentrations (0.2 mg/ml) produced some non-specific bands. This issue was resolved by reducing the nanobody concentration to 0.2 μ g/ml (Fig. S6). Next, we tested whether the two nanobodies could detect by immunoblotting proteins NanoTagged in different positions. NbVHH05 and Nb127D01 recognized proteins with internal, N- and C-terminal NanoTags on immunoblots (Fig. 3A). To test whether increasing the number of NanoTags improved the sensitivity of detection, we generated vectors that express secreted GFP with 1x, 2x or 3x-VHH05 or 127D01 Nanotags at the C-terminus (Fig. 3B). An N-terminal FLAG-tag was included in all constructs and used as the loading control. An increase in the number of NanoTags improved the sensitivity of detection using culture media that contain secreted GFP proteins (Fig. 3B). Tagging of target proteins with more than one copy of a tag thus improves the sensitivity of detection.

Next, we tested whether the nanobodies against the VHH05 and 127D01 tags could be used for multiplexed immunoblots by double-tagging the Upd2 cytokine (VHH05-Upd2-127D01). As we needed to detect each nanobody in a specific manner, we tagged one nanobody with the ALFA tag and detected it using NbALFA and the other, with a human IgG (hIgG). We expressed and purified nanobody-hIgG from S2 cells and tested different concentrations of conditioned media on immunoblots (Fig S7). Very dilute conditioned media still produced a strong signal, even though the nanobody-hIgG was not purified or concentrated. After establishing working concentrations of hIgG-tagged nanobody conditioned media, we performed multiplexed immunostaining using Nb127D01-hIgG and NbVHH05-ALFA, or NbVHH05-hIgG and Nb127D01-ALFA, detected with anti-human IgG and NbALFA, respectively (Fig. 3C). Upd2 undergoes fragmentation due to internal furin cleavage

sites, which produced different bands on the immunoblot. A combination of human IgG-tagged nanobody and ALFA-tagged nanobody can thus be used for multiplexed immunoblotting (Fig. 3C). In addition, we confirmed that a combination of NbVHH05-biotin and Nb127D01-hIgG also worked well for multiplexed immunoblotting (Fig. 3C).

Another key application of antibodies is immunopurification of target proteins. To explore whether NbVHH05 and Nb127D01 can be used for immunopurification, we coated NbALFA resin with ALFA-tagged VHH05 or 127D01 nanobodies and used the modified resin to recover NanoTagged FLAG-GFP secreted in S2 cell culture media. FLAG-GFP-3xVHH05 and FLAG-GFP-3x127D01 were captured by NbVHH05-ALFA and Nb127D01-ALFA, respectively (Fig. 3D and 3E). Protein A magnetic beads coated with Nb127D01-hIgG also successfully recovered FLAG-GFP-3x127D01 from S2 cell culture media (Fig. 3F). We confirmed that the VHH05 and 127D01 systems do not cross-react. (Fig. S5B). NanoTag-based immunopurification with these nanobodies is thus effective.

NanoTag trap as a method to alter protein localization

One of the many possible applications of nanobodies is to express them in cells or *in vivo* as fusion proteins localized to a particular subcellular location, in order to manipulate the localization of a NanoTagged POI. To test whether the NbVHH05/VHH05-tag and Nb127D01/127D01-tag can be used to alter localization, we constructed secreted GFP expression vectors that each had a N-terminal BiP signal peptide and a C-terminal VHH05- or 127D01-tag (BiP-GFP-VHH05 and BiP-GFP-127D01) (Fig. 4A and B). We also constructed NbVHH05 and Nb127D01 with mCherry and KDEL endoplasmic reticulum (ER) retention signal (BiP-Nanobody-mCherry-KDEL), which should result in retention of the fusion protein in the ER (Fig. 4A and B). When transfecting only BiP-GFP-VHH05 or BiP-GFP-127D01 into S2R+ cells, we did not observe GFP accumulation within cells, as the GFP fusion was actively secreted into the culture medium (Fig. 4C). However, after co-transfecting BiP-NbVHH05-mCherry-KDEL with BiP-GFP-VHH05, or BiP-Nb127D01-mCherry-KDEL with BiP-GFP-127D01, we observed intracellular accumulation of GFP that colocalized with the mCherry signal. This shows that NanoTagged-GFP proteins directed to the secretory pathway can be trapped by an ER NanoTag trap (i.e. nanobodies with an ER retention signal) (Fig. 4C). Indeed, cell lysates prepared from cells transfected with ER NanoTag trap showed more GFP signal on immunoblot, compared to controls lacking the ER NanoTag trap (Fig. 4D).

We also prepared membrane-tethered nanobodies (membrane NanoTag trap) in order to re-localize cytoplasmic NanoTagged proteins to the membrane (Fig. 4E and 4F). When S2R+ cells were co-transfected with CD8-NbVHH05-GFP/mito-mCherry-VHH05 or CD8-Nb127D01-GFP/mito-mCherry-127D01, mCherry colocalized with GFP on the cell membrane (Fig. 4G). NanoTag traps targeted to particular cellular compartments can thus alter the subcellular distribution of NanoTagged proteins. The ability to do so may facilitate a variety of functional analyses.

Assessing NanoTags *in vivo*

The successful use of the NbVHH05/VHH05-tag and Nb127D01/127D01-tag in cells prompted us to test them *in vivo*. We first constructed a series of UAS vectors with either a cytoplasmic or secreted version of the two nanobodies, tagged with GFP or HA (Fig. S8A), and tested them in cells. As expected, when transfected together with the *pAct-Gal4* plasmid, the cytoplasmic expression vectors led to an expression of nanobodies detectable in S2R+ cell lysates, and the secretory expression vectors resulted in detection of nanobodies predominantly in the culture media (Fig. S8B and S8C). Next, we generated transgenic flies carrying these UAS constructs. We did not expect NbVHH05 or Nb127D01 to interact with any fly endogenous proteins for lack of obvious sequence similarity between the *Drosophila* proteome and the amino acid sequence of the two tags (data not shown). To confirm this experimentally, we ubiquitously expressed NbVHH05 or Nb127D01 *in vivo* throughout development using *tubulin-Gal4*. The nanobodies were not toxic to flies; we readily obtained adult *tubulin-Gal4*, *UAS-Nanobody* flies and did not observe any detectable developmental defects or abnormalities (data not shown). To further test these constructs, we used fat body-specific *Lpp-Gal4* to drive NbVHH05 or Nb127D01 expression.

Immunofluorescence showed that GFP- or HA-tagged NbVHH05 or Nb127D01 is expressed at readily detectable levels in fat body cells (Fig. 4A-4D). We also confirmed that nanobodies with the BiP signal peptide are secreted (Fig. 4E and 4F).

To address whether NanoTagged POIs can be detected *in vivo*, we generated *UAS-VHH05-REPTOR-127D01* flies. A previous study has shown that in S2 cells, the transcription factor REPTOR is enriched in the cytoplasm under normal conditions but translocates into the nucleus upon rapamycin treatment (Tiebe et al., 2015). To test whether the changes in REPTOR localization can be detected using the nanobodies, we co-expressed NanoTagged REPTOR along with Nb127D01-GFP or NbVHH05-GFP specifically in adult enterocytes (ECs). In the absence of a NanoTagged POI, Nb127D01-GFP and NbVHH05-GFP were detected in both the cytoplasm and nuclei (Fig. 5G and 5I). In contrast, when co-expressed with NanoTagged REPTOR, the nanobody-GFP signals were enriched in the cytoplasm of ECs under normal food conditions (Fig. 5H and 5J). Following rapamycin treatment, a stronger GFP signal was observed in nuclei. Similar changes were absent from ECs that express Nb127D01-GFP or NbVHH05-GFP alone (Fig. 5G and 5I). These results confirm that rapamycin treatment leads to translocation of REPTOR into the nucleus *in vivo* and provide further support for the idea that co-expression of NanoTag POIs and nanobodies can visualize the subcellular location of a POI (Fig. 5H and 5J).

Next, we checked whether NanoTagged proteins can be detected *in vivo* using purified nanobodies. We first constructed several vectors that contain NanoTags at the N- or C-terminus of POIs and tested them in S2R+ cells. For secreted proteins, we replaced the endogenous signal peptide with the BiP signal peptide (Fig S8D). NanoTagged Akh, Dilp2, Dilp8, Pvf1, and Upd2 were readily detected in the culture media using NbVHH05 or Nb127D01 (Fig. S8E). REPTOR and two isoforms of REPTOR-BP (REPTOR-BP-B and REPTOR-BP-C) could also be detected using

NbVHH05 or Nb127D01 from transfected S2R+ cell lysates (Fig. S8F and G). In addition to *VHH05-REPTOR-127D01* flies, we also generated a version of *Upd2* with the BiP secretion signal and both NanoTags for *in vivo* study. We used *Myo1A^{ts}* to drive *UAS-BiP-VHH05-Upd2-127D01* and were able to detect the signal in adult midguts, using either NbVHH05 or Nb127D01 for detection by immunofluorescence (Fig. 5K-5N). Taken together, these data indicate that both NbVHH05/VHH05 and Nb127D01/127D01 work well for *in vivo* imaging and immunostaining.

CRISPR-mediated tagging of endogenous genes with NanoTags

In many cases, tagging endogenous proteins is preferable to UAS-based overexpression of tagged cDNAs, as UAS/Gal4-mediated expression can exceed physiological levels. Further, while many proteins have been tagged endogenously with GFP (Morin et al., 2001; Sarov et al., 2016; Li-Kroeger et al., 2018), tagging with smaller epitope tags may be preferable to minimize their structural impact. To tag endogenous genes with either VHH05-tag or 127D01-tag, we used a standard CRISPR-Cas9 targeted insertion method to tag fly proteins at their N- or C- terminus via the homology directed repair (HDR) pathway (Fig. 6A-C). To facilitate this approach, we first designed four universal vectors based on the scarless editing CRISPR knock-in approach (Lamb et al., 2017). Each vector contains four common features: *3xP3-dsRed-SV40* for identification of transformants, 5'/3' terminal repeats for piggyBac transposase recognition sequences, TTAA for piggyBac target sequence, and an EcoRI restriction site for cloning target locus homologous arms by Gibson assembly (Fig. 6A'). We chose Histone H2A variant (H2Av) as an example, because the expected nuclear localization of H2Av should be easily visualized. We cloned the sequence 1 kb upstream and 1 kb downstream of the stop codon (TAA) into the donor vector. An sgRNA plasmid that targeted a seed sequence near the TAA of H2Av gene was injected into *yw; nos-cas9/CyO* embryos together with the donor plasmid (Fig. 6B'). Positive transformants with red fluorescent eyes were outcrossed and successful knock-in events were confirmed by junction PCR and sequencing. Subsequently, 3xP3dsRed was excised using piggyBac transposase (Fig. 6C'). After sequence verification (Fig. S9), we immunostained midguts from H2Av-3x127D01- and H2Av-3xVHH05-expressing flies using Nb127D01-HA or NbVHH05-HA. As shown in Fig. 6D' and Fig. S10, H2Av tagged with either NanoTag was clearly observed in the nucleus, demonstrating that this tagging method can be used effectively to engineer NanoTagged forms of POIs and study their localization and/or function at physiological expression levels.

DISCUSSION

In this study, we characterized two NanoTags, VHH05 and 127D01, and their corresponding nanobodies, for use in *Drosophila* for cellular and *in vivo* studies. We show that these two systems can be used for *in vivo* detection via CBs, re-localization, direct or indirect immunostaining, immunoblotting, and immunopurification. The observation that these nanobodies recognize the NanoTags on immunoblots is particularly useful, as only few nanobodies that recognize a defined amino acid

sequence have been characterized as suitable for immunoblotting (Cheloha et al., 2020) The utility of this system is further enhanced by ease of purification of nanobodies from either bacterial cells or *Drosophila* cultured cells. Modification of these nanobodies with ALFA or HA tags facilitates detection. Installation of a human Fc portion on these nanobodies enables the use of anti-IgG antibodies as secondary reagents for detection. In addition, we used chemical labeling or site-specific sortase labeling to prepare nanobodies labeled with fluorophores or biotin. We have thus developed reagents with broad applicability in *Drosophila* research and beyond.

The system described here has significant advantages over conventional antibodies or anti-GFP nanobodies. Nanobodies, unlike conventional antibodies, are easily encoded as a single open reading frame in the genomes of model organisms or cells. In addition, the small size of the NanoTags may be preferable in many cases to GFP, as GFP is bulky and may affect the function of the tagged protein. Also, the relatively long protein maturation time of GFP limit its use for imaging nascent proteins. Finally, the anti-GFP nanobody, as used in deGradFP (Caussinus et al., 2011), only poorly recognizes unfolded GFP.

We show how these short tags can be introduced into endogenous genes, using the scarless CRISPR knock-in editing approach. Given the small size of the tags, additional methods for genome modification deserve to be explored. For example, ssDNA based CRISPR knock-in can be used to insert short sequences into a precise location in the genome (Ling et al., 2017). Another possibility is prime editing, which relies on pegRNAs to insert sequences smaller than 48 bp into a chosen genomic position (Anzalone et al., 2019; Bosch et al., 2021).

A key feature of the NanoTag/nanobody system is the ability to co-express the nanobody *in vivo* in the form of a CB or some other fusion. We show that this approach can be used to re-localize proteins. Expression *in vivo* also opens the doors to using versions of the deGrad system or other functional fusions to manipulate proteins in other ways (Caussinus and Affolter, 2016). Some S2R+ cells transfected with Nb127D01-GFP contained aggregates (data not shown). However, we did not observe aggregates in Nb127D01-mCherry transfected cells or transgenic Nb127D01-GFP flies, nor did we observe developmental defects or effects on viability following expression of the tags and/or nanobodies *in vivo*. The occasional observation of protein aggregation in cells more likely reflects the high level of expression when transfecting cells with exogenous expression constructs.

Given their versatility and *in vivo* applications, we anticipate that the two NanoTags and corresponding nanobodies will be useful to address many cell biological questions. The relative ease with which the system can be used for *in vivo* tagging, as well as our demonstration that the system can be used in a number of ways for imaging (i.e. using CBs or direct or indirect immunofluorescence) are obvious assets. The NanoTag approach might be particularly useful for the new and growing need to spatially map cell clusters identified from scRNAseq studies (Mohr et al., 2021). Other potential applications for *in vivo* tagged proteins include chromosome immunoprecipitation (ChIP), immunopurification of protein complexes,

and inducing degradation of proteins that carry the tag (e.g. as shown for GFP in Caussinus et al., 2011; Neumuller et al., 2012).

Although we developed and validated the NanoTag system for use in *Drosophila*, the same approaches should be applicable to other systems. The mouse genome contains a predicted amino acid sequence with 100% identity to the epitope recognized by VHH05, which is not surprising, given that the tag sequence is identical to a segment of the human source protein, Ube6e. For 127D01, however, no proteins encoded by the mouse genome have peptides with more than 50% identity to the tag, suggesting that 127D01 could be used for murine studies. Moreover, there are no peptides with more than 50% identity to either tag in many species of research interest, including *E. coli*, *Saccharomyces cerevisiae*, *C. elegans*, *Arabidopsis thaliana*, *Oryza sativa* (rice), the mosquitoes *Aedes aegypti*, *Anopheles gambiae* and *Anopheles stephensi*, *Bombyx mori* (silkworm), *Tribolium castaneum* (red flour beetle), *Danaus plexippus* (monarch butterfly), and *Danio rerio* (zebrafish), suggesting that both tags could be used in these organisms.

METHODS

Plasmids

Four types of vectors were used in this study: 1. pAW, that contains the fly actin5C promoter; 2. pWalium10, a UAS/Gal4 vector that contains a UAS promoter and mini-white selection marker (DGRC, 1470); 3. pMT (pMK-33GW, Ram Viswanatha); and 4. pET-26b (Novagen 69862). pAW-HGP-sortase is a pAW vector derivative with N-terminal BiP signal peptide/FLAG-tag, AarI-cloning site for Gibson or HiFi assembly, C-terminal purification tag with Sortase-tag and His-tag, and heat shock promoter-GFP-T2A-PuroR for stable cell line generation. pMT-HGP-v3 is a pMT vector derivative with N-terminal BiP signal peptide/FLAG-tag, AarI-cloning site for Gibson or HiFi assembly, C-terminal purification tag with Avi-tag and His-tag, and heat shock promoter-GFP-T2A-PuroR for stable cell line generation. pET-26b-Nb-GGA is a pET-26b derivative with BsaI Golden Gate Assembly cloning site flanked by pelB signal sequence and C-terminal ALFA- and His-tags.

Plasmid DNAs were constructed and amplified using standard protocols. Briefly, plasmids were linearized by restriction enzymes as described by the commercial vendor. PCR fragments were amplified using Phusion polymerase (New England Biolabs (NEB), M0530) or Q5 polymerase (NEB, M0494). Linearized plasmids and PCR fragments were gel purified using QIAquick columns (Qiagen, #28115) and joined using either Gibson assembly (NEB, E2611) or NEBuilder HiFi assembly (NEB, E2621). Reactions were transformed into chemically competent TOP10 *Escherichia coli* (Invitrogen, C404010), plated and selected on lysogeny broth (LB)-agar plates with ampicillin (100 µg/mL) or kanamycin (50 µg/mL). Colony PCR was performed using Takara Taq polymerase (Clontech, TAKR001C). Plasmid DNA was isolated from cultured bacteria using QIAprep Spin Miniprep Kit (Qiagen, 27104). Plasmid sequences were confirmed by Sanger sequencing performed at the

Dana-Farber/Harvard Cancer Center DNA Resource Core or Genewiz. Primers sequences are listed in Table S1.

pW10-Nanobody variants. All UAS constructs were cloned into the pWalium10 (pW10) vector. For pW10-NbVHH05-HA, pW10-Nb127D01-HA, pW10-NbVHH05-GFP, pW10-Nb127D01-GFP, pW10-BiP-NbVHH05-HA, pW10-BiP-Nb127D01-HA, pW10-BiP-NbVHH05-GFP, and pW10-BiP-Nb127D01-GFP, pW10 was first linearized with EcoRI (NEB, R0101) and XbaI (NEB, R0145). NbVHH05 or Nb127D01 were cloned from pHEN6-VHH05 or pHEN6-127D01 (Ploegh lab). GFP was amplified from PXL-IE1-EGFP-nos-Cas9 (Xu et al., 2020). PCR fragments were joined together with the digested pW10 backbone by Gibson assembly. HA and BiP were incorporated by adding overhanging sequences to the primers. For pW10-BiP-VHH05-Akh-127D01, pW10-BiP-VHH05-Dilp2-127D01, pW10-BiP-VHH05-Dilp8-127D01, pW10-BiP-VHH05-Pvf1-127D01 and pW10-BiP-VHH05-Upd2-127D01, pW10 was first digested with EcoRI and XbaI. A BiP-VHH05-127D01 fragment was made by annealing two oligos and ligated into the linearized pW10 to generate the intermediate vector, pW10-BiP-VHH05-BglIII-127D01. Next, PCR fragments of *Akh*, *Dilp2*, *Dilp8*, *Pvf1*, and *Upd2* were amplified from fly cDNAs and inserted into pW10-UAS-BiP-VHH05-127D01 linearized by BglIII (NEB, R0144) by Gibson assembly. For pW10-127D01-REPTOR-bp-B-VHH05, pW10-127D01-REPTOR-bp-C-VHH05 and pW10-127D01-REPTOR-VHH05, pW10-BiP-VHH05-127D01 was digested with EcoRI and BglIII to remove BiP-VHH05. VHH05 was introduced N-terminal of PCR fragments of *REPTOR-bp-B*, *REPTOR-bp-C* and *REPTOR* through overhanging primers. PCR fragments were inserted into pW10-127D01 (EcoRI and BglIII digested) by Gibson assembly.

pAW-Nanobody/NanoTagged fluorophore variants. For pAW-NbVHH05-GFP, pAW-Nb127D01-GFP, pAW-NbVHH05-mCherry, pAW-Nb127D01-mCherry, pAW-H2B-mCherry-VHH05, pAW-H2B-mCherry-127D01, pAW-mito-mCherry-VHH05, pAW-mito-mCherry-127D01, pAW-CD8-mCherry-VHH05, pAW-CD8-mCherry-127D01, pAW-VHH05-H2B-mCherry, pAW-127D01-H2B-mCherry, pAW-BiP-NbVHH05-mCherry-KDEL, pAW-BiP-Nb127D01-mCherry-KDEL, pAW-CD8-NbVHH05-GFP and pAW-CD8-Nb127D01-GFP, pAW was first linearized with NheI (NEB, R3131) and XbaI. NbVHH05-GFP and Nb127D01-GFP were amplified from pW10-NbVHH05-GFP and pW10-Nb127D01-GFP. *CD8*, *mCherry* and *CD8-mCherry* were cloned from pQUASp-mCD8mCherry (Addgene, #46164). *H2B-mCherry* was cloned from pBac (3xP3-gTc'v; pUb:lox-mYFP-lox-H2BmCherry) (Addgene, #119064). *mito-mCherry* was cloned from pcDNA4TO-mito-mCherry-10xGCN4_v4 (Addgene, #60914). BiP-NbVHH05 or BiP-Nb127D01 fragments were cloned from pW10-UAS-BiP-NbVHH05-GFP, pW10-UAS-BiP-Nb127D01-GFP. PCR fragments were joined together with the digested pAW backbone by Gibson assembly. VHH05-, 127D01-tags, or KDEL sequences were incorporated in the N- or C-terminus by adding overhanging sequences to the primers. For pAW-CD8-VHH05-mCherry and

pAW-CD8-127D01-mCherry, we first digested pAW-CD8-mCherry-VHH05 with NheI to obtain a linearized pAW-CD8 backbone. mCherry was amplified from pQUASp-mCD8mCherry. VHH05 or 127D01 was introduced into the N-terminal of PCR fragments with overhanging primer sequences. The NanoTag-mCherry PCR fragment was inserted into pAW-CD8 by Gibson assembly.

pAW-HGP-BiP-GFP with 1x/2x/3x NanoTags. For pAW-HGP-BiP-GFP-VHH05, pAW-HGP-BiP-GFP-2xVHH05, pAW-HGP-BiP-GFP-3xVHH05, pAW-HGP-BiP-GFP-127D01, pAW-BiP-HGP-GFP-2x127D01, pAW-HGP-BiP-GFP-3x127D01, pAW-HGP-sortase was first linearized by AarI (Thermo Scientific ER1581). N-terminal GFP was amplified by PCR. C-terminal GFP with 1x/2x/3x NanoTags were prepared by gene synthesis (Twist Bioscience). PCR fragment and C-terminal GFP with NanoTags were joined together with the linearized pAW-HGP-sortase by NEBuilder HiFi assembly.

pMT-HGP-v3-Nb127D01-hlgG, pMT-HGP-v3-NbVHH05-hlgG. For cloning of the inducible Nb127D01-hlgG and NbVHH05-hlgG expression vectors, the pMT-HGP-v3 vector was linearized by both AarI and NsiI-HF (NEB, R3127). Human IgG Fc region was amplified from pCER243 (a gift of Aaron Ring at Yale). NbVHH05/Nb127D01 and hlgG PCR fragments were inserted into pMT-HGP-v3 (digested by AarI and NsiI-HF) by NEBuilder HiFi assembly.

pET-26b-Nb127D01-ALFA-His, pET-26b-NbVHH05-ALFA-His, pET-26b-Nb127D01-HA-His, pET-26b-NbVHH05-HA-His. For cloning pET-26b-Nb127D01-ALFA-His and pET-26b-NbVHH05-ALFA-His, NbVHH05/Nb127D01 PCR fragments were cloned into pET-26b-Nb-GGA by BsaI-Golden Gate Assembly (NEB, E1601). To make pET-26b-Nb127D01-HA-His and pET-26b-NbVHH05-HA-His, NbVHH05/Nb127D01 PCR fragments with HA tag were cloned into pET-26b (NcoI, NEB, R3193 and XhoI, NEB, R0146 digested) by HiFi assembly.

pScarless NanoTag vectors: pScarlessHD-C-3x127D01-DsRed, pScarlessHD-C-3xVHH05-DsRed, pScarlessHD-N-3x127D01-DsRed, pScarlessHD-N-3xVHH05-DsRed. 3x127D01 or 3xVHH05 were cloned from pAW-HGP-BiP-GFP-3x127D01 or pAW-HGP-BiP-GFP-3xVHH05. 3xP3-DsRed was cloned from pScarlessHD-2xHA-DsRed (Addgene, 80822). Then, 3x127D01 or 3xVHH05 and 3xP3-DsRed PCR fragments were inserted into pScarlessHD-2xHA-DsRed backbone (EcoRI digested) by Gibson assembly.

pScarlessHD-C-3x127D01-H2Av-DsRed, pScarlessHD-C-3xVHH05-H2Av-DsRed. pScarlessHD-C-3x127D01-DsRed and pScarlessHD-C-3xVHH05-DsRed were digested with EcoRI to obtain the pScarlessHD backbone and 3xP3-DsRed fragment. Upstream and downstream sequences of TAA at the C-terminus of the H2Av gene were cloned from *yw*; *nos-Cas9/Cyo* flies. Then, 3xP3-DsRed, upstream and downstream fragments were inserted into pScarlessHD backbone by Gibson assembly.

pCFD3-H2Av-sgRNA. pCFD3 (Addgene, #49410) was digested with BbsI (NEB, R0539). sgRNA oligos following phosphorylation were annealed by T4PNK (NEB,

M0201) and inserted into a digested pCFD3 backbone by T4 DNA ligase (NEB, M0202).

Cell transfection

Drosophila S2R+ cells were cultured at 25°C in Schneider's media (Thermo Fisher Scientific, 21720-024) with 10% fetal bovine serum (Sigma, A3912) and 50 U/mL penicillin-streptomycin (Thermo Fisher Scientific, 15070-063). S2R+ cells were transfected using Effectene (Qiagen, 301427) following the manufacturer's instructions. A total of 200ng of plasmid DNA per well was transfected 24-well plates. The culture medium was replaced 24 hours after transfection.

To produce secreted GFP proteins with 1x/2x/3x NanoTags and Nanobodies with human IgG, ESF921-adapted S2 cells (Expression Systems, 94-005S) were transfected using PEI transfection methods and cultured in protein-free ESF921 media (Expression Systems, 96-001). For 6-well plate transfection, 2.4µg of DNA and 7.4µg of PEI were mixed in 300µl of ESF921 media for 15-30 min and added to 2.7ml of S2 cell culture (2E6 cells/ml, final cell density). Alternatively, 50ml suspension cells cultured in 250ml flask were transfected using the same proportion. On day 2 from transfection, protein expression was induced with 700µM CuSO₄ for 5 days. Cleared conditioned media were collected after centrifugation and directly used for immunostaining, western blot, and immunoprecipitation.

Fly Strains

Fly husbandry and crosses were performed under standard conditions at 25°C. Injections were carried in-house. Fly strains used to generate transgenic lines were attP lines: attP40 (*y,v; P{nos- phiC31\int.NLS}X; P{CaryP}attP40*) and attP2 (*y,w; P{nos- phiC31\int.NLS}X; P{CaryP}attP2*). Fly strains used to generate KI lines were *y,w; nos-Cas9/CyO*. For balancing chromosomes, fly stocks *y,w; TM3, Sb/TM6, Tb, yw; Gla/CyO, yw; If/CyO; MKRS/TM6, Tb* were used. All lines recovered were homozygous viable. Fly stocks are from the Perrimon fly stock unless stated otherwise. Other fly stocks used in this study were *Lpp-Gal4* (Hong-Wen Tang) and *Myo1A-Gal4, tub-Gal80^{ts}* (Afroditi Petsakou).

Generating transgenic flies

Transgenic flies generated in this study are as follows:

yw; UAS-NbVHH05-HA, w+ attp2
yw; UAS-NbVHH05-HA, w+ attp40
yw; UAS-Nb127D01-HA, w+ attp2
yw; UAS-Nb127D01-HA, w+ attp40
yw; UAS-NbVHH05-GFP, w+ attp2
yw; UAS-NbVHH05-GFP, w+ attp40
yw; UAS-Nb127D01-GFP, w+ attp2
yw; UAS-Nb127D01-GFP, w+ attp40
yw; UAS-BiP-NbVHH05-HA, w+ attp2
yw; UAS-BiP-NbVHH05-HA, w+ attp40

yw; UAS-BiP-Nb127D01-HA, w+ attp2
yw; UAS-BiP-Nb127D01-HA, w+ attp40
yw; UAS-BiP-NbVHH05-GFP, w+ attp2
yw; UAS-BiP-NbVHH05-GFP, w+ attp40
yw; UAS-BiP-Nb127D01-GFP, w+ attp2
yw; UAS-BiP-Nb127D01-GFP, w+ attp40
yw; UAS-BiP-VHH05-Upd2-127D01, w+ attp40
yw; UAS-VHH05-REPTOR-127D01, w+ attp40
w; H2Av-3xVHH05/TM3, Sb
w; H2Av-3x127D01/TM3, Sb

Transgenic flies were generated by phiC31 integration of attB-containing plasmids into either attP40 or attP2 landing sites. Briefly, plasmid DNA was purified on QIAquick columns and eluted in injection buffer (100 μ M NaPO₄, 5 mM KCl) at a concentration of 200-400 ng/ μ L. Plasmid DNA was injected into ~100 fertilized embryos (*y,v nos-phiC31int; attP40* or *y,w nos-phiC31int; attP2*) through microinjection handle (NARISHIGE, Japan) with pressure control (FemtoJet, Eppendorf). The progeny was outcrossed to screen for transgenic founder progeny and the UAS insertions were isolated by screening for white+ eye color.

To generate KI flies, donor and sgRNA plasmids were mixed together and were injected into ~100 fertilized embryos (*y,w; nos-Cas9/CyO*). Transformed lines were isolated using a DsRed marker. To remove the DsRed cassette, transformed lines were crossed to a line expressing PBac transposase (BL #8285). Resulting lines were sequenced to confirm the insertion of 3x127D01 or 3xVHH05 to the C-terminal of the *H2Av* gene.

Targeted integration analysis

Genomic DNA was extracted from the DsRed2-positive G1 adult animals by standard sodium dodecyl sulfate (SDS) lysis-phenol buffer after incubation with proteinase K (Roche, 3115879001), followed by RNase A (Thermo Fisher Scientific, EN0531) treatment and purification. The 5'- and 3'-end junction fragments at the integration event were cloned separately and sequenced. PCR conditions included 2 min of denaturation at 95 °C; 30 cycles of 1 min at 95 °C, 30 s at 55 °C and 1min at 72 °C; followed by a final extension at 72 °C for 10 min by using Takara Taq polymerase (Clontech, #TAKR001). To remove the DsRed cassette, the genomic DNA was extracted by the same method and PCR conditions included 2 min of denaturation at 95 °C; 30 cycles of 1 min at 95 °C, 30 s at 55 °C and 30 s at 72 °C; followed by a final extension at 72 °C for 10 min. PCR products were sub-cloned into the pJET-1.2 vector (Fermentas, #K1231) and sequenced. Primer sequences are listed in the Table S1.

Rapamycin treatment

For rapamycin treatment, rapamycin (LC Laboratories, R-5000) was dissolved in DMSO and mixed into the media when preparing food vials. The rapamycin dose was 50uM.

Nanobody purification

Nanobody expression vectors with C-terminal ALFA-tag or HA-tag for bacterial expression and purification were cloned into pET-26b-Nb-GGA or pET-26b by Golden-Gate assembly or Gibson cloning, respectively. After transformation with BL21 (DE3) competent cells (NEB, C25271), overnight cultures were inoculated in LK media and incubated at 37°C until the OD600 approached ~0.6. Then, 0.1mM IPTG was added and cultures were placed at 15°C for overnight. After centrifugation, the cell pellet was collected and resuspended in B-PER II Bacterial Protein Extraction Reagent (Thermo Scientific, 78260). After 30 min incubation with rotation, an additional 19X volume of TBS was added and further incubated with rotation. Cleared supernatants were collected after centrifugation at 20,000 g & 4°C for 15 min and used for His-tag purification. Dialyzed His-tag purified nanobody fractions were diluted at 0.2mg/ml concentration, which were directly used for immunostainings and western blots. To generate fluorescent-labeled nanobodies, Mix-n-Stain CF 555 Antibody Labeling Kit and Mix-n-Stain CF 647 Antibody Labeling Kit (Sigma-Aldrich, MX555S100 and MX647S100) were used according to the manufacturer's protocol.

Nanobodies equipped with an LPETGG motif and a His-tag at their C-terminus were functionalized with triglycine containing probes using Sortase 5M as previously described (Cheloha et al., 2019). Briefly, LPETGG motif and His-tag at the C-terminus of nanobodies were replaced with fluorophore or biotin contained in triglycine probes by sortagging reaction. Ni-NTA resin (EMD Millipore, 70691-3) was used to remove unreacted His-tagged nanobodies and His-tagged Sortase 5M enzyme, and the flow-through (sortase-based labeled nanobodies) was collected. The flow-through was applied to PD-10 column (GE Healthcare, GE17-0851-01) to remove excess triglycine probes.

Immunostaining and imaging analysis

Drosophila fat body and midguts from adult females were fixed in 4% paraformaldehyde in Phosphate-buffered saline (PBS) at room temperature for 1 hour, incubated for 1 hour in Blocking Buffer (5% Normal Donkey Serum, 0.3% Triton X-100, 0.1% Bovine serum albumin (BSA) in PBS), and stained with primary antibodies overnight at 4°C in PBST (0.3% Triton X-100, 0.1% BSA in PBS). S2R+ cells were fixed in 4% paraformaldehyde in PBS at room temperature for 30 minutes, incubated for 1 hour in Blocking Buffer, and stained with primary antibodies for 2-3 hours at room temperature in PBST. The primary antibodies and their dilutions used are: NbVHH05-ALFA (1:500), NbVHH05-HA (1:500), NbVHH05-hIgG (1:20, S2 cell culture media), NbVHH05-555 (1:500), Nb127D01-ALFA (1:500), Nb127D01-HA (1:500), Nb127D01-hIgG (1:20, S2 cell culture media), Nb127D01-647 (1:500), mouse anti-GFP (Invitrogen, A11120; 1:300), rat anti-HA (Sigma-Aldrich, 3F10; 1:1000). After primary antibody incubation, the fat body and midguts or S2R+ cells were washed 3 times with PBST, stained with 4',6-diamidino-2-phenylindole (DAPI) (1:2000 dilution) and Alexa Fluor-conjugated donkey-anti-mouse, donkey-anti-rabbit and mouse-anti-human IgG secondary antibodies (Molecular Probes, 1:1000), or

NbALFA-Atto647 (NanoTag Biotechnologies, N1502-At647N-L; 1:500) Goat Anti-Alpaca IgG-647 (Jackson ImmunoResearch, 128-605-230; 1:500) in PBST at 22°C for 2 hours, washed 3 times with PBST, and mounted in Vectashield medium.

All images of the posterior midgut or S2R+ cells that are presented in this study are confocal images captured with a Nikon Ti2 Spinning Disk confocal microscope. Z-stacks of 5-20 images covering one layer of the epithelium from the apical to the basal side were obtained, adjusted, and assembled using NIH Fiji (ImageJ), and shown as a maximum projection.

Western blots

Cultured cells were harvested 3 days after transfection. For fly, 6-8 larval fat bodies or 3 female midguts per group were dissected in PBS, placed in 50µl lysis buffer (Pierce, #87788) with 2x protease and phosphatase inhibitor cocktail (Pierce, #78440) and 2 mM trypsin inhibitor benzamidine (Sigma-Aldrich, #434760), and homogenized using Kimble Kontes pellet pestles (Millipore, Z359947). Protein lysates were incubated in 2xSDS sample buffer (Thermo Scientific, #39001) containing 5% 2-Mercaptoethanol at 100°C for 10 minutes, ran on a 4%-20% polyacrylamide gel (Bio-Rad, #4561096), and transferred to an Immobilon-P polyvinylidene fluoride (PVDF) membrane (Millipore, IPVH00010). The membrane was blocked by 5% BSA or 5% skim milk in 1x Tris-buffered saline (TBS) containing 0.1% Tween-20 (TBST) at room temperature for 30 minutes. The following primary antibodies were used: anti-tubulin (Sigma, T5168, 1:10,000), rabbit anti-GFP (Molecular Probes, A-6455; 1:10000) and anti-FLAG M1 (Sigma, F3040, 1:5,000), rat anti-HA (Sigma-Aldrich, 3F10; 1:10000), NbVHH05 (0.2mg/ml, 1:5000, or 1:100~1:100000 used in concentration gradient test), Nb127D01 (0.2mg/ml, 1:5000, or 1:100~1:100000 used in concentration gradient test), NbVHH05-hIgG (1:100, S2 cell culture media), Nb127D01-hIgG (1:100, S2 cell culture media) in blocking solution. After washing with TBST, signals were detected with enhanced chemiluminescence (ECL) reagents (Amersham, RPN2209; Pierce, #34095) or fluorescent secondary antibody information. Western blot images were acquired by Bio-Rad ChemiDoc MP or X-ray film exposure.

Immunoprecipitation

For immunoprecipitation using ALFA-tagged nanobodies (NbVHH05-ALFA and Nb127D01-ALFA), His-tag purified nanobodies from bacteria were incubated with ALFA Selector ST resin (Nanotag Biotechnologies, N1511) at room temperature for 1 hour. The resin was washed with Pierce IP lysis buffer (Thermo Scientific, 87787) (3X) and incubated with S2 cell culture media containing secreted GFP proteins with 3xVHH05-tag and 3x127D01-tag at 4°C for 1 hour. After washing in IP lysis buffer (4X), proteins were eluted in 2x sample buffer.

For immunoprecipitation using human IgG-formatted nanobody (Nb127D01-hIgG), Protein A Magnetic Beads (Bio-Rad, 1614013) were incubated with S2 cell culture media containing Nb127D01-hIgG at room temperature for 1 hour. After washing in IP lysis buffer (3X), beads were incubated with the conditioned media

containing secreted GFP proteins 3x127D01-tag at 4°C for 1 hour. After washing in IP lysis buffer (4X), proteins were eluted in 2x sample buffer.

ELISA

GFP fused at its C-terminus with a peptide corresponding to the extracellular portion of human CXCR2 (full-length, Supplementary Figure 1), produced through sortagging, was immobilized on Nunc 96-well Maxisorp flat bottom plates (100 ng/well). After immobilization, wells were blocked using a solution of BSA in PBS (5% w/v). Nb127D01 conjugated with biotin (20 nM) was mixed with peptides corresponding to full-length CXCR2 extracellular domain or two fragments at varying concentrations. These solutions were then added to plates with immobilized GFP-CXCR2 and incubated for 1 h. These solutions were discarded from the plates, the plates were washed with PBS containing 0.05% Tween-20, and the amount of Nb127D01-biotin bound to the plate was quantified through the addition of streptavidin-HRP (Thermo Fisher, N100), washing, and the addition of tetramethylbenzidine-containing solution (Thermo Fisher, N301).

QUANTIFICATION AND STATISTICAL ANALYSIS

Data are presented as the mean \pm SEM (Fig. S1). Western blot signal is quantified by ImageJ (Fig. 3B).

ACKNOWLEDGMENTS

We thank the assistance provided by the Microscopy Resources on the North Quad (MicRoN) core at Harvard Medical School and Christians Villalta for help with the generation of transgenic flies. This work was supported by NIH NIGMS P41 GM132087. J.S.S. L. is supported by a Croucher fellowship for Postdoctoral Research from the Croucher Foundation. N.P. is an investigator of Howard Hughes Medical Institute.

AUTHOR CONTRIBUTIONS

J.X., A.R. K. and N.P. conceptualized and designed the experiments. J.X. and A.R. K. performed most of the experiments. R.W. C., F.A. F., H. P., J.S.S. L., Y. F., E. S. and R. B. contributed reagents and helped with experiments. J.X., A.R. K., R. W. C. and N.P. analyzed the data. J.X. and A.R. K. wrote the paper (original draft). J.S.S. L., S.E. M., J. Z., R. W. C., H. P. and N.P. edited the paper. All authors discussed the results and commented on the paper.

DECLARATION OF INTERESTS

The authors declare no competing interests.

KEY RESOURCES TABLE

REAGENT or RESOURCE	SOURCE	IDENTIFIER
Antibodies, nanobodies		
Mouse anti- α -Tubulin	Sigma-Aldrich	Cat# T5168; RRID: AB_477579
Mouse anti-GFP	Invitrogen	Cat# A11120; RRID: AB_221568
Rat anti-HA	Sigma-Aldrich	Cat# 3F10; RRID: AB_2314622
Mouse anti-FLAG M1	Sigma-Aldrich	Cat# F3040; RRID: AB_439712
NbALFA-HRP	NanoTag Biotechnologies	Cat# N1502-HRP
NbALFA-Atto647	NanoTag Biotechnologies	Cat# N1502-At647N-L
NbALFA-800CW	NanoTag Biotechnologies	Cat# N1502-Li800-L
Goat Anti-Alpaca IgG-647	Jackson ImmunoResearch	Cat# 128-605-230
Mouse anti-HA-Alexa Fluor 488	Thermo Fisher Scientific	Cat# A-21287
Goat Anti-Human IgG Fc-HRP	Thermo Fisher Scientific	Cat# A18829
Donkey anti-Human IgG-DyLight 680	Thermo Fisher Scientific	Cat# SA5-10130
Streptavidin-DyLight 800	Thermo Fisher Scientific	Cat# 21851
Streptavidin-Alexa Fluor 488	Thermo Fisher Scientific	Cat# S32354
NbVHH05-HA	This paper	N/A
NbVHH05-ALFA	This paper	N/A
NbVHH05-hIgG	This paper	N/A
NbVHH05-555	This paper	N/A
NbVHH05-biotin (sortagging)	This paper	N/A
NbVHH05 -555 (sortagging)	This paper	N/A
Nb127D01-HA	This paper	N/A
Nb127D01-ALFA	This paper	N/A
Nb127D01-hIgG	This paper	N/A
Nb127D01-647	This paper	N/A
Chemicals, Peptides, and Recombinant Proteins		
Proteins		
Phusion polymerase	New England Biolabs	Cat# M0530
Q5 polymerase	New England Biolabs	Cat# M0494
Taq polymerase	Clontech	Cat# TAKR001
EcoRI	New England Biolabs	Cat# R0101
XbaI	New England Biolabs	Cat# R0145
BglII	New England Biolabs	Cat# R0144
NheI	New England Biolabs	Cat# R3131
NsiI-HF	New England Biolabs	Cat# R3127
NcoI-HF	New England Biolabs	Cat# R3193
XhoI	New England Biolabs	Cat# R0146
BbsI	New England Biolabs	Cat# R0539

Aarl	Thermo Fisher Scientific	Cat# ER1581
T4PNK	New England Biolabs	Cat# M0201
T4 DNA ligase	New England Biolabs	Cat# M0202
fetal bovine serum	Sigma-Aldrich	Cat# A3912
Schneider's media	Thermo Fisher Scientific	Cat# 21720-024
penicillin-streptomycin	Thermo Fisher Scientific	Cat# 15070-063
ESF921 media	Expression Systems	Cat# 96-001
proteinase K	Roche	Cat# 3115879001
RNase A	Thermo Fisher Scientific	Cat# EN0531
protease and phosphatase inhibitor cocktail	Pierce	Cat# 78440
trypsin inhibitor benzamidine	Sigma-Aldrich	Cat# 434760
4',6-diamidino-2-phenylindole (DAPI)	Thermo Fisher Scientific	Cat# D1306
rapamycin	LC Laboratories	Cat# R-5000
HRP-Conjugated Streptavidin	Thermo Fisher Scientific	Cat# N100
Critical Commercial Assays		
Gibson assembly	New England Biolabs	Cat# E2611
NEBuilder HiFi assembly	New England Biolabs	Cat# E2621
Golden Gate Assembly	New England Biolabs	Cat# E1601
pJET-1.2 vector kit	Fermentas	Cat# K1231
QIAquick Gel Extraction Kit	Qiagen	Cat# 28706
QIAquick Spin Columns	Qiagen	Cat# 28115
Effectene	Qiagen	Cat# 301427
B-PER II Bacterial Protein Extraction Reagent	Thermo Fisher Scientific	Cat# 78260
Mix-n-Stain CF 555 Antibody Labeling Kit	Sigma-Aldrich	Cat# MX555S100
Mix-n-Stain CF 647 Antibody Labeling Kit	Sigma-Aldrich	Cat# MX647S100
Ni-NTA resin	EMD Millipore	Cat# 70691-3
PD-10 column	GE Healthcare	Cat# GE17-0851-01
lysis buffer	Pierce	Cat# 87788
SDS sample buffer	Thermo Fisher Scientific	Cat# 39001
4%-20% polyacrylamide gel	Bio-Rad	Cat# 4561096
enhanced chemiluminescence (ECL) reagents	Amersham	Cat# RPN2209
enhanced chemiluminescence (ECL) reagents	Pierce	Cat# 34095
ALFA Selector ST resin	Nanotag Biotechnologies	Cat# N1511
Pierce IP lysis buffer	Thermo Fisher Scientific	Cat# 87787
Protein A Magnetic Beads	Bio-Rad	Cat# 1614013
tetramethylbenzidine-containing solution	Thermo Fisher Scientific	Cat# N301

Plasmids		
pAW	Perrimon lab	N/A
pWalium10	DGRC	Cat# 1470
pMK-33GW	Perrimon lab	N/A
pET-26b	Novagen	Cat# 69862
pQUASp-mCD8mCherry	Addgene	Cat# 46164
pBac (3xP3-gTc'v; pUb:lox-mYFP-lox-H2BmCherry)	Addgene	Cat# 119064
pcDNA4TO-mito-mCherry-10xGCN4_v4	Addgene	Cat# 60914
PXL-IE1-EGFP-nos-Cas9	Xu et al., 2020	N/A
pScarlessHD-2xHA-DsRed	Addgene	Cat# 80822
pCFD3	Addgene	Cat# 49410
pAW-NbVHH05-GFP	This paper	N/A
pAW-Nb127D01-GFP	This paper	N/A
pAW-NbVHH05-mCherry	This paper	N/A
pAW-Nb127D01-mCherry	This paper	N/A
pAW-H2B-mCherry-VHH05	This paper	N/A
pAW-mito-mCherry-VHH05	This paper	N/A
pAW-CD8-mCherry-VHH05	This paper	N/A
pAW-H2B-mCherry-127D01	This paper	N/A
pAW-mito-mCherry-127D01	This paper	N/A
pAW-CD8-mCherry-127D01	This paper	N/A
pAW-VHH05-H2B-mCherry	This paper	N/A
pAW-CD8-VHH05-mCherry	This paper	N/A
pAW-127D01-H2B-mCherry	This paper	N/A
pAW-CD8-127D01-mCherry	This paper	N/A
pAW-BiP-NbVHH05-mCherry-KDEL	This paper	N/A
pAW-BiP-Nb127D01-mCherry-KDEL	This paper	N/A
pAW-CD8-NbVHH05-GFP	This paper	N/A
pAW-CD8-Nb127D01-GFP	This paper	N/A
pAW-HGP-BiP-FLAG-GFP-VHH05	This paper	N/A
pAW-HGP-BiP-FLAG-GFP-2xVHH05	This paper	N/A
pAW-HGP-BiP-FLAG-GFP-3xVHH05	This paper	N/A
pAW-HGP-BiP-FLAG-GFP-127D01	This paper	N/A
pAW-HGP-BiP-FLAG-GFP-2x127D01	This paper	N/A
pAW-HGP-BiP-FLAG-GFP-3x127D01	This paper	N/A
pW10-UAS-BiP-127D01-Akh-VHH05	This paper	N/A
pW10-UAS-BiP-127D01-Dilp2-VHH05	This paper	N/A

pW10-UAS-BiP-127D01-Dilp8-VHH05	This paper	N/A
pW10-UAS-BiP-127D01-Pvf1-VHH05	This paper	N/A
pW10-UAS-127D01-REPTOR-bp-B-VHH05	This paper	N/A
pW10-UAS-127D01-REPTOR-bp-C-VHH05	This paper	N/A
pMT-HGP-v3-Nb127D01-hlgG	This paper	N/A
pMT-HGP-v3-NbVHH05-hlgG	This paper	N/A
pET-26b-Nb127D01-HA-His	This paper	N/A
pET-26b-NbVHH05-HA-His	This paper	N/A
pET-26b-Nb127D01-ALFA-His	This paper	N/A
pET-26b-NbVHH05-ALFA-His	This paper	N/A
pW10-UAS-NbVHH05-HA	This paper	N/A
pW10-UAS-BiP-NbVHH05-HA	This paper	N/A
pW10-UAS-Nb127D01-HA	This paper	N/A
pW10-UAS-BiP-Nb127D01-HA	This paper	N/A
pW10-UAS-NbVHH05-GFP	This paper	N/A
pW10-UAS-BiP-NbVHH05-GFP	This paper	N/A
pW10-UAS-Nb127D01-GFP	This paper	N/A
pW10-UAS-BiP-Nb127D01-GFP	This paper	N/A
pW10-UAS-127D01-REPTOR-VHH05	This paper	N/A
pW10-UAS-BiP-127D01-Upd2-VHH05	This paper	N/A
pW10-UAS-BiP-127D01-Akh-VHH05	This paper	N/A
pCFD3-H2Av-sgRNA	This paper	N/A
pScarlessHD-C-3x127D01-H2Av-DsRed	This paper	N/A
pScarlessHD-C-3xVHH05-H2Av-DsRed	This paper	N/A
pScarlessHD-C-3x127D01-DsRed	This paper	N/A
pScarlessHD-C-3xVHH05-DsRed	This paper	N/A
pScarlessHD-N-3x127D01-DsRed	This paper	N/A
pScarlessHD-N-3xVHH05-DsRed	This paper	N/A

Experimental Models: Cell Lines

S2R+	DGRC	Cat# 150
ESF921-adapted S2 cells	This paper	N/A

Experimental Models: Organisms/Strains

w1118	Perrimon lab	N/A
y,v; P{nos- phiC31\int.NLS}X; P{CaryP}attP40	Perrimon lab	N/A
y,w; P{nos- phiC31\int.NLS}X; P{CaryP}attP2	Perrimon lab	N/A
y,w; nos-Cas9/CyO	Perrimon lab	N/A

y,w; TM3, Sb/TM6,Tb	Perrimon lab	N/A
yw; Gla/CyO	Perrimon lab	N/A
yw; If/CyO; MKRS/TM6, Tb	Perrimon lab	N/A
Myo1A-Gal4, tub-Gal80 ^{ts}	Perrimon lab	N/A
Lpp-Gal4	Perrimon lab	N/A
yw; UAS-NbVHH05-HA, w+ attp2	This paper	N/A
yw; UAS-NbVHH05-HA, w+ attp40	This paper	N/A
yw; UAS-Nb127D01-HA, w+ attp2	This paper	N/A
yw; UAS-Nb127D01-HA, w+ attp40	This paper	N/A
yw; UAS-NbVHH05-GFP, w+ attp2	This paper	N/A
yw; UAS-NbVHH05-GFP, w+ attp40	This paper	N/A
yw; UAS-Nb127D01-GFP, w+ attp2	This paper	N/A
yw; UAS-Nb127D01-GFP, w+ attp40	This paper	N/A
yw; UAS-BiP-NbVHH05-HA, w+ attp2	This paper	N/A
yw; UAS-BiP-NbVHH05-HA, w+ attp40	This paper	N/A
yw; UAS-BiP-Nb127D01-HA, w+ attp2	This paper	N/A
yw; UAS-BiP-Nb127D01-HA, w+ attp40	This paper	N/A
yw; UAS-BiP-NbVHH05-GFP, w+ attp2	This paper	N/A
yw; UAS-BiP-NbVHH05-GFP, w+ attp40	This paper	N/A
yw; UAS-BiP-Nb127D01-GFP, w+ attp2	This paper	N/A
yw; UAS-BiP-Nb127D01-GFP, w+ attp40	This paper	N/A
yw; UAS-BiP-VHH05-Upd2-127D01, w+ attp40	This paper	N/A
yw; UAS-VHH05-REPTOR-127D01, w+ attp40	This paper	N/A
w; H2Av-3xVHH05/TM3, Sb	This paper	N/A
w; H2Av-3x127D01/TM3, Sb	This paper	N/A
TOP10 <i>Escherichia coli</i>	Invitrogen	Cat# C404010
BL21 (DE3) <i>Escherichia coli</i>	New England Biolabs	Cat# C25271
Oligonucleotides		
All oligos	This paper	See Table S1
Software		
Photoshop	Adobe	N/A
ImageJ	NIH	N/A
Excel	Microsoft	N/A
GraphPad Prism6	GraphPad	N/A
Other		
Joystick Micromanipulator	NARISHIGE	Cat# MN-151

FemtoJet Microinjector	Eppendorf	Cat# LV41365120
Garfunkel Nikon Ti2 Spinning Disk	Nikon	N/A
Kimble Kontes pellet pestles	Millipore	Cat# Z359947
Immobilon-P polyvinylidene fluoride (PVDF) membrane	Millipore	Cat# IPVH00010
ChemiDoc MP imaging system	Bio-Rad	Cat# 17001402
Kodak M35 X-OMAT Automatic Processors	KODAK	Cat# RT-KP-M35A
Hyperfilm™ ECL™	Amersham	Cat# GE28-9068-35

CONTACT FOR REAGENT AND RESOURCE SHARING

Further information and requests for resources and reagents should be directed to and will be fulfilled by the Lead Contact, Norbert Perrimon (perrimon@genetics.med.harvard.edu).

REFERENCES

- Aguilar, G., Matsuda, S., Vigano, M.A., and Affolter, M. (2019). Using Nanobodies to Study Protein Function in Developing Organisms. *Antibodies (Basel)* 8, 16.
- Anzalone, A.V., Randolph, P.B., Davis, J.R., Sousa, A.A., Koblan, L.W., Levy, J.M., Chen, P.J., Wilson, C., Newby, G.A., Raguram, A., and Liu, D.R. (2019). Search-and-replace genome editing without double-strand breaks or donor DNA. *Nature* 576, 149–157.
- Boersma, S., Khuperkar, D., Verhagen, B.M.P., Sonneveld, S., Grimm, J.B., Lavis, L.D., and Tanenbaum, M.E. (2019). Multi-Color Single-Molecule Imaging Uncovers Extensive Heterogeneity in mRNA Decoding. *Cell* 178, 458–472.
- Bosch, J.A., Birchak, G., and Perrimon, N. (2021). Precise genome engineering in *Drosophila* using prime editing. *Proc. Natl. Acad. Sci. USA* 118, e2021996118.
- Bradley, M.E., Dombrecht, B., Manini, J., Willis, J., Vlerick, D., De Taeye, S., Van den Heede, K., Roobrouck, A., Grot, E., Kent, T.C., Laeremans, T., Steffensen, S., Van Heeke, G., Brown, Z., Charlton, S.J., and Cromie, K.D. (2015). Potent and efficacious inhibition of CXCR2 signaling by biparatopic nanobodies combining two distinct modes of action. *Mol. Pharmacol.* 87, 251–262.
- Caussinus, E., and Affolter, M. (2016). deGradFP: A System to Knockdown GFP-Tagged Proteins. *Methods Mol. Biol.* 1478, 177–187.
- Caussinus, E., Kanca, O., and Affolter, M. (2011). Fluorescent fusion protein knockout mediated by anti-GFP nanobody. *Nat. Struct. Mol. Biol.* 9, 117–121.

Cheloha, R.W., Harmand, T.J., Wijne, C., Schwartz, T.U., and Ploegh, H.L. (2020). Exploring cellular biochemistry with nanobodies. *J. Biol. Chem.* *295*, 15307–15327.

Cheloha, R.W., Li, Z., Bousbaine, D., Woodham, A.W., Perrin, P., Volarić, J., and Ploegh, H.L. (2019). Internalization of Influenza Virus and Cell Surface Proteins Monitored by Site-Specific Conjugation of Protease-Sensitive Probes. *ACS Chem. Biol.* *14*, 1836–1844.

De Genst, E.J., Guilliams, T., Wellens, J., O'Day, E.M., Waudby, C.A., Meehan, S., Dumoulin, M., Hsu, S.T., Cremades, N., Verschueren, K.H., Pardon, E., Wyns, L., Steyaert, J., Christodoulou, J., and Dobson, C.M. (2010). Structure and properties of a complex of α -synuclein and a single-domain camelid antibody. *J. Mol. Biol.* *402*, 326–343.

Fang, T., Lu, X., Berger, D., Gmeiner, C., Cho, J., Schalek, R., Ploegh, H., and Lichtman, J. (2018). Nanobody immunostaining for correlated light and electron microscopy with preservation of ultrastructure. *Nat. Methods.* *15*, 1029–1032.

Fornasiero, E.F., and Opazo, F. (2015). Super-resolution imaging for cell biologists: concepts, applications, current challenges and developments. *Bioessays* *37*, 436–451.

Götzke, H., Kilisch, M., Martínez-Carranza, M., Sograte-Idrissi, S., Rajavel, A., Schlichthaerle, T., Engels, N., Jungmann, R., Stenmark, P., Opazo, F., and Frey, S. (2019). The ALFA-tag is a highly versatile tool for nanobody-based bioscience applications. *Nat. Commun.* *10*, 4403.

Guimaraes, C.P., Witte, M.D., Theile, C.S., Bozkurt, G., Kundrat, L., Blom, A.E., and Ploegh, H.L. (2013). Site-specific C-terminal and internal loop labeling of proteins using sortase-mediated reactions. *Nat. Protoc.* *8*, 1787–1799.

Harmansa, S., Alborelli, I., Bieli, D., Caussinus, E., and Affolter, M. (2017). A nanobody-based toolset to investigate the role of protein localization and dispersal in *Drosophila*. *Elife* *6*, e22549.

Harmansa, S., and Affolter, M. (2018). Protein binders and their applications in developmental biology. *Development* *145*, dev148874.

Helma, J., Cardoso, M.C., Muyldermans, S., and Leonhardt, H. (2015). Nanobodies and recombinant binders in cell biology. *J. Cell. Biol.* *209*, 633–644.

Harmansa, S., Hamaratoglu, F., Affolter, M., and Caussinus, E. (2015). Dpp spreading is required for medial but not for lateral wing disc growth. *Nature* *527*, 317–322.

Lamb, A.M., Walker, E.A., and Wittkopp, P.J. (2017). Tools and strategies for scarless allele replacement in *Drosophila* using CRISPR/Cas9. *Fly (Austin)* *11*, 53–64.

Ling, J., Cheloha, R.W., McCaul, N., Sun, Z.J., Wagner, G., and Ploegh, H.L. (2019). A nanobody that recognizes a 14-residue peptide epitope in the E2 ubiquitin-conjugating enzyme UBC6e modulates its activity. *Mol. Immunol.* *114*, 513–523.

Ling, L., Kokoza, V.A., Zhang, C., Aksoy, E., and Raikhe, A.S. (2017). MicroRNA-277 targets insulin-like peptides 7 and 8 to control lipid metabolism and reproduction in *Aedes aegypti* mosquitoes. *Proc. Natl. Acad. Sci. USA* *114*, E8017–E8024.

Li-Kroeger, D., Kanca, O., Lee, P.T., Cowan, S., Lee, M.T., Jaiswal, M., Salazar, J.L., He, Y., Zuo, Z., and Bellen, H.J. (2018). An expanded toolkit for gene tagging based on MiMIC and scarless CRISPR tagging in *Drosophila*. *Elife* *7*, e38709.

Mikhaylova, M., Cloin, B.M., Finan, K., van den Berg, R., Teeuw, J., Kijanka, M.M., Sokolowski, M., Katrukha, E.A., Maidorn, M., Opazo, F., Moutel, S., Vantard, M., Perez, F., van Bergen en Henegouwen, P.M., Hoogenraad, C.C., Ewers, H., and Kapitein, L.C. (2015). Resolving bundled microtubules using anti-tubulin nanobodies. *Nat. Commun.* *6*, 7933.

Mohr, S.E., Tattikota, S.G., Xu, J., Zirin, J., Hu, Y., and Perrimon, N. (2021). Methods and tools for spatial mapping of single-cell RNAseq clusters in *Drosophila*. *Genetics* *217*, iyab019.

Morin, X., Daneman, R., Zavortink, M., and Chia, W. (2001). A protein trap strategy to detect GFP-tagged proteins expressed from their endogenous loci in *Drosophila*. *Proc. Natl. Acad. Sci. USA* *98*, 15050–15055.

Neumüller, R.A., Wirtz-Peitz, F., Lee, S., Kwon, Y., Buckner, M., Hoskins, R.A., Venken, K.J., Bellen, H.J., Mohr, S.E., and Perrimon, N. (2012). Stringent analysis of gene function and protein-protein interactions using fluorescently tagged genes. *Genetics* *190*, 931–940.

Sarov, M., Barz, C., Jambor, H., Hein, M.Y., Schmied, C., Suchold, D., Stender, B., Janosch, S., K J, V.V., Krishnan, R.T., Krishnamoorthy, A., Ferreira, I.R., Ejsmont, R.K., Finkl, K., Hasse, S., Kämpfer, P., Plewka, N., Vinis, E., Schloissnig, S., Knust, E., Hartenstein, V., Mann, M., Ramaswami, M., VijayRaghavan, K., Tomancak, P., and Schnorrer, F. (2016). A genome-wide resource for the analysis of protein localisation in *Drosophila*. *Elife* *5*, e12068.

Tanenbaum, M.E., Gilbert, L.A., Qi, L.S., Weissman, J.S., and Vale, R.D. (2014). A protein-tagging system for signal amplification in gene expression and fluorescence imaging. *Cell* *159*, 635–646.

Tiebe, M., Lutz, M., De La Garza, A., Buechling, T., Boutros, M., and Teleman, A.A. (2015). REPTOR and REPTOR-BP Regulate Organismal Metabolism and Transcription Downstream of TORC1. *Dev. Cell.* *33*, 272–284.

Traenkle, B., Emele, F., Anton, R., Poetz, O., Haeussler, R.S., Maier, J., Kaiser, P.D., Scholz, A.M., Nueske, S., Buchfellner, A., Romer, T., and Rothbauer, U. (2015). Monitoring interactions and dynamics of endogenous beta-catenin with intracellular nanobodies in living cells. *Mol. Cell Proteomics* *14*, 707–723.

Vigano, M.A., Ell, C.M., Kustermann, M.M.M., Aguilar, G., Matsuda, S., Zhao, N., Stasevich, T.J., Affolter, M., and Pyrowolakis, G. (2021). Protein manipulation using single copies of short peptide tags in cultured cells and in *Drosophila melanogaster*. *Development* 148, dev191700.

Virant, D., Traenkle, B., Maier, J., Kaiser, P.D., Bodenhofer, M., Schmees, C., Vojnovic, I., Pisak-Lukáts, B., Endesfelder, U., and Rothbauer, U. (2018). A peptide tag-specific nanobody enables high-quality labeling for dSTORM imaging. *Nat Commun.* 9, 930.

Wang, S., Tang, N.H., Lara-Gonzalez, P., Zhao, Z., Cheerambathur, D.K., Prevo, B., Chisholm, A.D., Desai, A., and Oegema, K. (2017). A toolkit for GFP-mediated tissue-specific protein degradation in *C. elegans*. *Development* 44, 2694–2701.

Xu, J., Liu, W., Yang, D., Chen, S., Chen, K., Liu, Z., Yang, X., Meng, J., Zhu, G., Dong, S., Zhang, Y., Zhan, S., Wang, G., and Huang, Y. (2020). Regulation of olfactory-based sex behaviors in the silkworm by genes in the sex-determination cascade. *PLoS Genet.* 16, e1008622.

Yamaguchi, N., Colak-Champollion, T., and Knaut, H. (2019). zGrad is a nanobody-based degron system that inactivates proteins in zebrafish. *Elife* 8, e43125.

Zhao, N., Kamijo, K., Fox, P.D., Oda, H., Morisaki, T., Sato, Y., Kimura, H., and Stasevich, T.J. (2019). A genetically encoded probe for imaging nascent and mature HA-tagged proteins in vivo. *Nat. Commun.* 10, 2947.

Figure legends

Figure 1. VHH05 and 127D01 NanoTag sequences and their corresponding nanobodies, and use of nanobodies as chromobodies. (A and C) VHH05 and 127D01 were inserted at the N-terminus, internally or at the C-terminus of a protein of interest (POI). GSG denotes the linker, M is the start codon, and Stop is the stop codon. (B and D) Nanobody sequences of NbVHH05 and Nb127D01. Bolded and underlined CDR1-3 correspond to complementarity-determining regions (CDRs). (E) Co-transfection of pAW-actin5C-NbVHH05-GFP and pAW-actin5C-VHH05-H2B-mCherry into S2R⁺ cells. H2B is a nuclear protein. (F) Co-transfection of pAW-actin5C-NbVHH05-GFP and pAW-actin5C-CD8-VHH05-mCherry into S2R⁺ cells. CD8 is a cell membrane protein (G) Co-transfection of pAW-actin5C-NbVHH05-GFP and pAW-actin5C-mito-mCherry-VHH05 into S2R⁺ cells. Mito-mCherry-VHH05 contains a localization signal peptide for mitochondrial outer membrane targeting. (H, I and J) Experiments are as in E, F and G, except that pAW-actin5C-Nb127D01-GFP and pAW-actin5C-127D01-H2B-mCherry were co-transfected.

Figure 2. Using NbVHH05 and Nb127D01 for immunofluorescence. (A)

Fluorophore-conjugated NbVHH05 or Nb127D01 recognizes VHH05- or 127D01-tagged fluorescence proteins. (A') VHH05- or 127D01-tagged mito-GFP can be detected by the corresponding NbVHH05-555 or Nb127D01-647 in transfected

S2R+ cells. (B) Schematic of nanobodies containing ALFA-tag as primary antibody and NbALFA as a secondary antibody. (B') VHH05- or 127D01-tagged mito-GFP can be detected using the corresponding nanobodies in transfected S2R+ cells. (C) Schematic of fluorophore-conjugated anti-Alpaca IgG antibodies to detect VHH05- and 127D01-tagged proteins. NbVHH05 or Nb127D01 are used as primary antibodies and anti-Alpaca IgG as secondary antibody. (C') VHH05- or 127D01-tagged mito-GFP can be detected using the corresponding nanobodies and anti-Alpaca IgG-647 in transfected S2R+ cells. (D) Schematic of using VHH05 and 127D01 for double tagging. N-, C-terminal of REPTOR contains VHH05 and 127D01. (D') Co-straining NbVHH05 and Nb127D01 in S2R+ cells transfected with VHH05-REPTOR-127D01.

Figure 3. Detection of tagged target proteins by western blotting and immunoprecipitation. (A) Lysates from S2R+ cells, transfected with different tagged plasmids (as used in Figure 1) or a mock control plasmid, were analyzed by SDS-PAGE and western blotting. The blot was developed with NbVHH05 and Nb127D01 followed by NbALFA-HRP or a mouse anti-tubulin primary antibody followed by anti-Mouse IgG HRP. (B) Schematics depict VHH05- or 127D01-tagged secreted GFP proteins bound by NbVHH05-ALFA and Nb127D01-ALFA followed by NbALFA-HRP. Culture media from S2R+ cells transfected with secreted BiP-GFP-1xtag, BiP-GFP-2xtag, BiP-GFP-3xtag were used for the western blotting. Anti-FLAG antibody was used to show the GFP level. Histogram showing the relative gray value of anti-NbVHH05 or anti-Nb127D01 to anti-FLAG. Plasmid information is in Supplementary Fig. 6. (C) Western blots for S2R+ cell culture media containing Upd2 double-tagged protein: N- and C-terminus region of Upd2 contains VHH05 and 127D01, respectively, recognized by NbVHH05 or Nb127D01. The secondary antibodies were anti-HlgG-HRP, anti-ALFA-800, and Streptavidin-800. (D) Immunoprecipitation of FLAG-GFP-3xVHH05 using NbVHH05-ALFA and ALFA-resin. The control nanobody failed to capture FLAG-GFP-3xVHH05. (E) Immunoprecipitation of FLAG-GFP-3x127D01 using Nb127D01-ALFA and ALFA-resin. (F) Immunoprecipitation of FLAG-GFP-3x127D01 using Nb127D01-hlgG and Protein A magnetic bead.

Figure 4. Nanobody-based system for altering localization of NanoTagged proteins. (A and B) Diagram showing the vectors used for the secreted protein trapping method. NbVHH05/Nb127D01 fused to mCherry contains KDEL and BiP signal peptide and is driven by the actin5C promoter. (C) Four independent cell transfection experiments were performed. In 1 and 3, only GFP-VHH05 or GFP-127D01 was transfected. In 2 and 4, NbVHH05-mCherry-KDEL with GFP-VHH05, or Nb127D01-mCherry-KDEL with GFP-127D01, were co-transfected. Images show the GFP and mCherry signal 48 hours after transfection. Nuclei are stained with DAPI. (D) Immunoblots of GFP and tubulin in cell lysates from transfections 1-4. (E and F) Diagram showing the vectors used for cytoplasmic protein trapping. NbVHH05/Nb127D01 is fused to GFP and CD8, and driven by actin5C promoter. Target proteins are mCherry containing VHH05 or 127D01 at the

C-terminus and mito signal at the N-terminus. (G) Results of co-transfection of CD8-NbVHH05-GFP/mito-mCherry-VHH05 and CD8-Nb127D01-GFP/mito-mCherry-127D01 in S2R+ cells. DAPI, GFP, mCherry and merge channels show protein expression levels with antibody stainings.

Figure 5. Nanobodies expression *in vivo*. (A-D) *Lpp-Gal4* drives fat body expression of *UAS-NbVHH05-GFP*, *UAS-NbVHH05-HA*, *UAS-Nb127D01-GFP*, or *UAS-Nb127D01-HA*, detected by GFP or anti-HA immunostaining. (E and F) Western blot detection of cytoplasmic and secreted GFP- or HA-tagged nanobodies. Lysates from fat body or hemolymph were tested by anti-GFP, anti-HA and anti-tubulin antibodies. Cytoplasmic-expressed nanobodies: *UAS-NbVHH05-GFP*, *UAS-Nb127D01-GFP*, *UAS-NbVHH05-HA* and *UAS-Nb127D01-HA*. Secreted-expressed nanobodies: *UAS-BiP-NbVHH05-GFP*, *UAS-BiP-Nb127D01-GFP*, *UAS-BiP-NbVHH05-HA* and *UAS-BiP-Nb127D01-HA*. (G-J) Confocal images of *Drosophila* adult guts expressing 127D01-EGFP/VHH05-GFP and VHH05-REPTOR-127D01 with or without rapamycin (Rapa) treatment for 15 hours. REPTOR shuttles into the nucleus upon Rapa treatment. G and I as controls only express 127D01-EGFP or VHH05-GFP in the ECs. H combines 127D01-EGFP with VHH05-REPTOR-127D01 and J combines VHH05-EGFP with VHH05-REPTOR-127D01. (K-N) Immunostaining of double tag-labeled proteins. K and L are control Oregon-R flies stained with NbVHH05 and Nb127D01. M and N are stained with NbVHH05 and Nb127D01 in the gut of flies carrying *UAS-BiP-VHH05-Upd2-127D01* driven by *Myo1A^{ts}*. Red box indicates an enlarged area of the gut.

Figure 6. Endogeneous VHH05- or 127D01-tagging using CRISPR/Cas9.

Workflow (A), fly embryos transformation (B), genotyping (C), and applications (D). (A') Common scarless vectors used for constructing donors. N-terminal vectors (PHD-N-3x127D01-donor or PHD-N-3xVHH05-donor) and C-terminal vectors (PHD-C-3x127D01-donor or PHD-C-3xVHH05-donor) contain EcoRI restriction enzyme sites that introduce the homologous arm sequences into donors. (B') Workflow example for introducing knock-in (KI) tags into the third chromosome. (C') Genotyping example of KI 3xVHH05 and 3x127D01 into the C-terminus of H2Av. Gel results showing the 5' and 3' PCR junctions. Representative sequencing chromatogram of PCR products from the junction PCR. (D') Immunostaining of H2Av-3x127D01 and H2Av-3xVHH05. Adult male or female guts were dissected and stained with Nb127D01-HA or NbVHH05-HA.

Figure 1

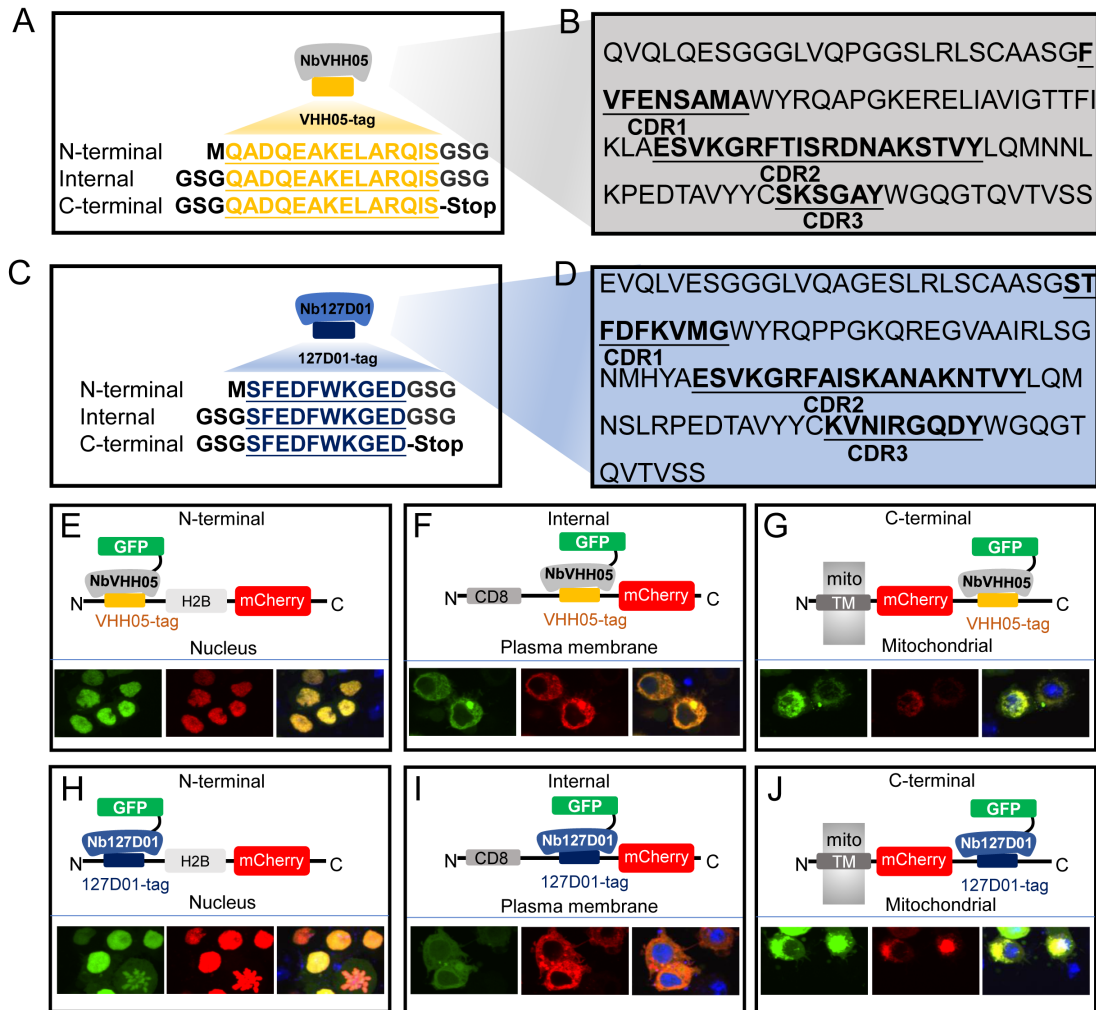


Figure 2

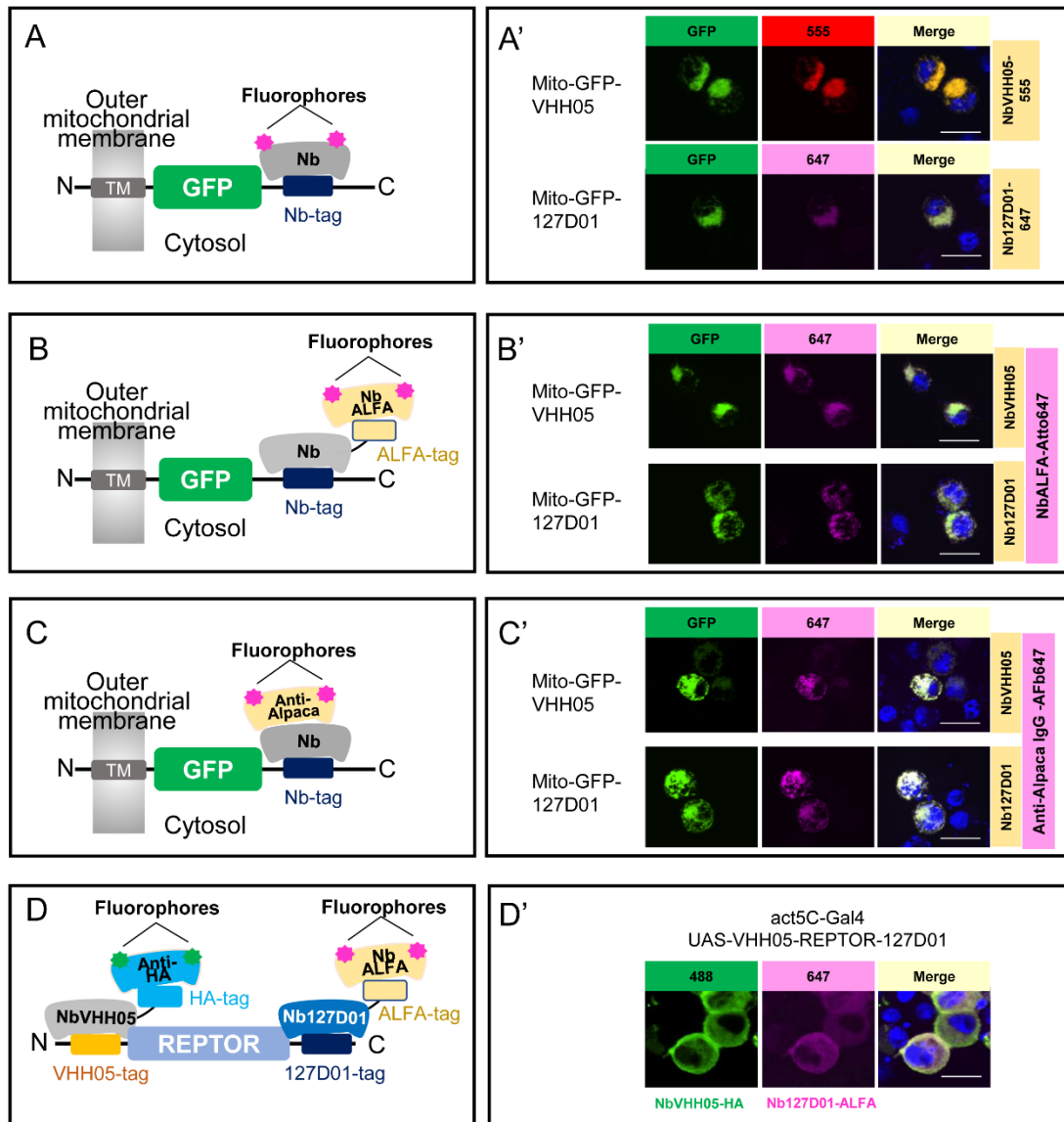


Figure 3

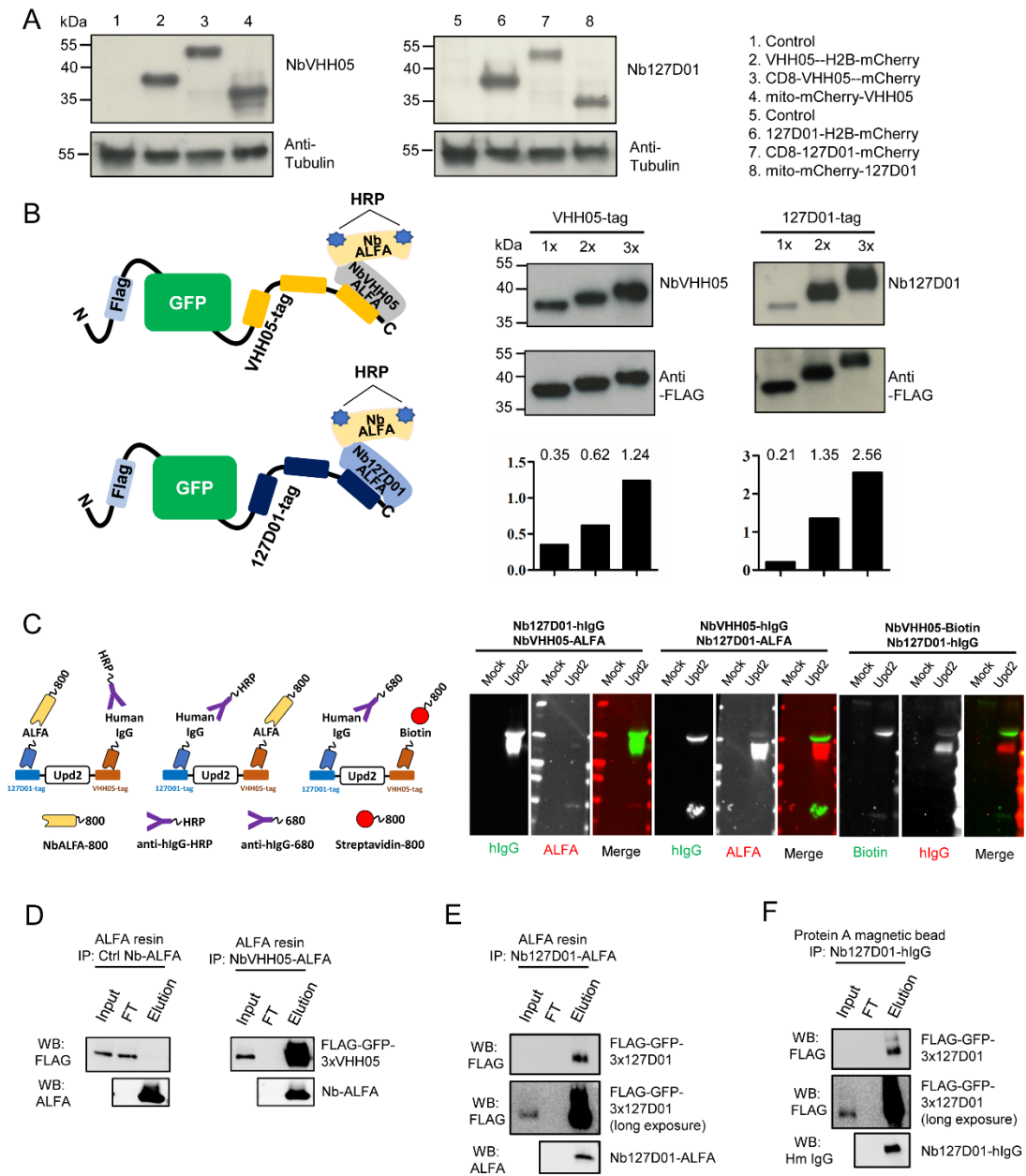


Figure 4

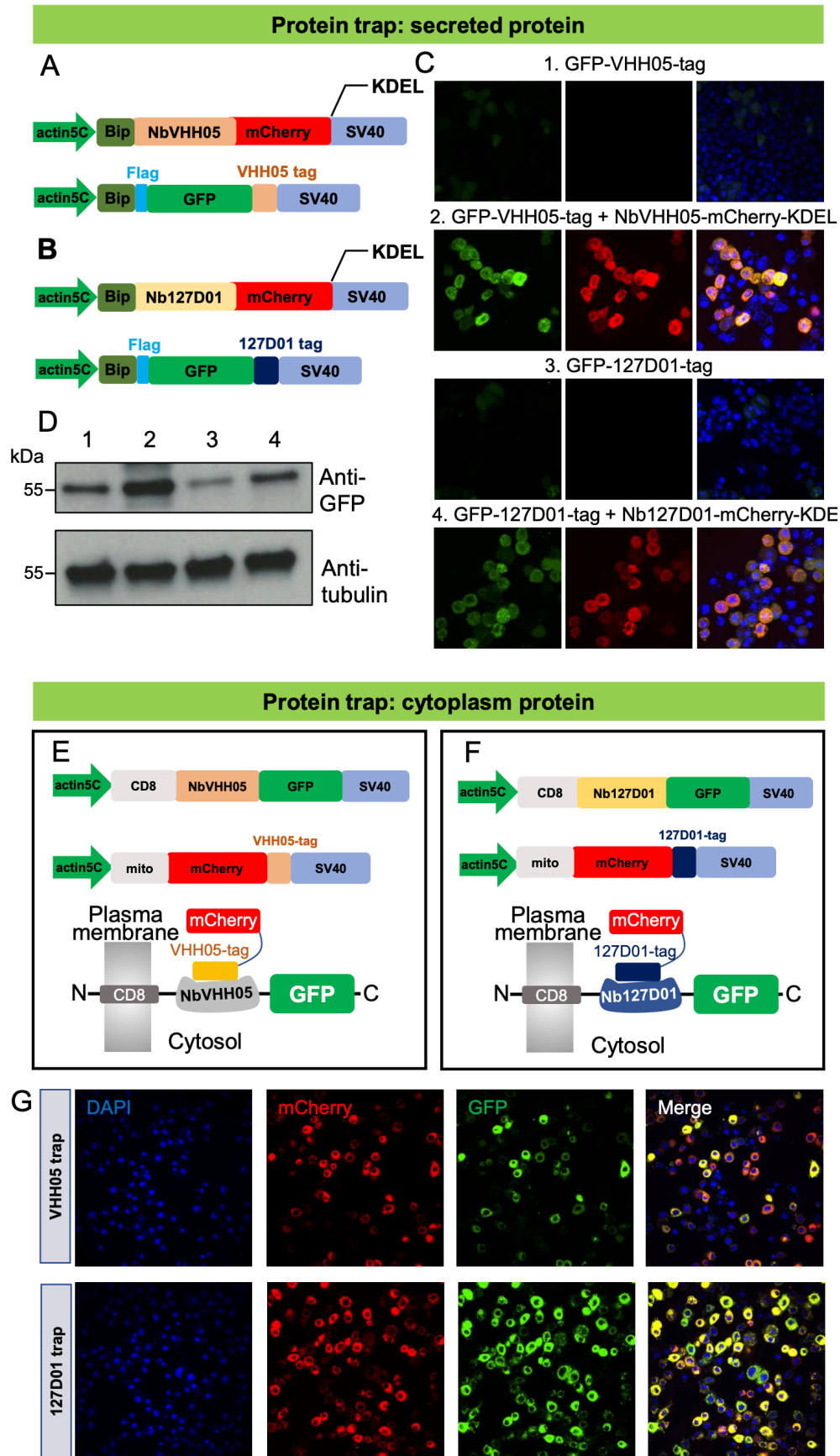


Figure 5

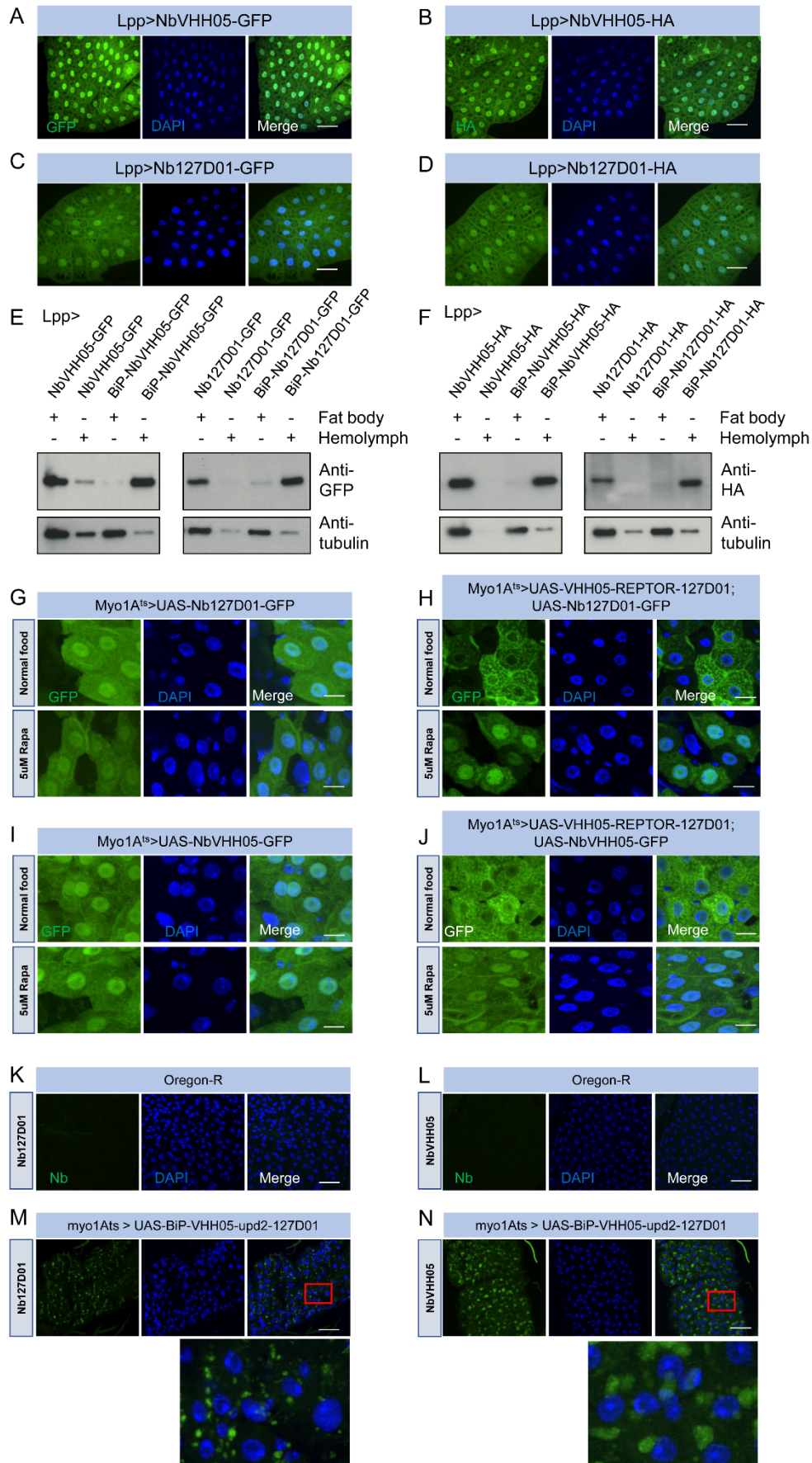
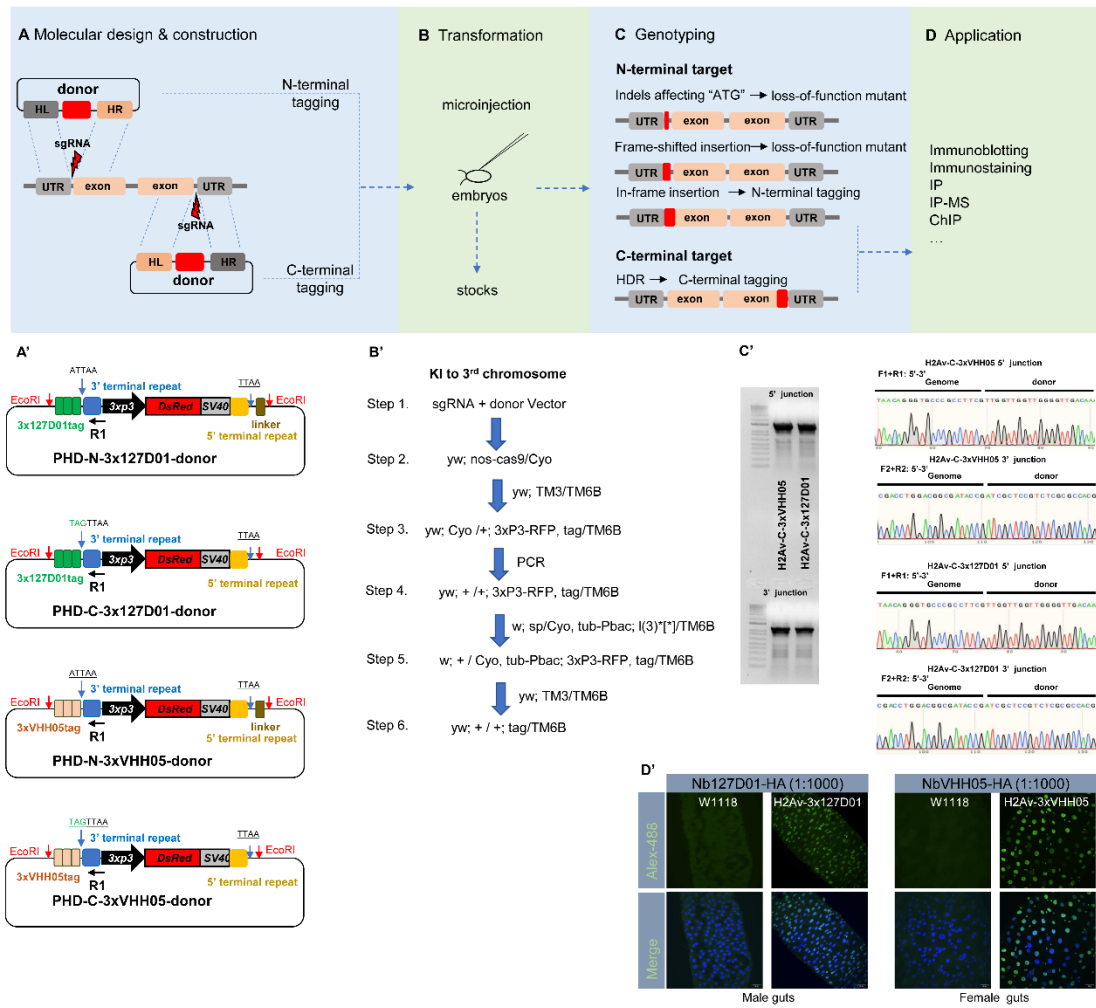


Figure 6



Supplemental Information

Protein visualization and manipulation in *Drosophila* through the use of epitope tags recognized by nanobodies (NanoTags)

Jun Xu, Ah-Ram Kim, Ross W. Cheloha, Fabian A. Fischer, Joshua Shing Shun Li, Yuan Feng, Emily Stoneburner, Richard Binari, Stephanie E. Mohr, Jonathan Zirin, Hidde Ploegh and Norbert Perrimon

Supplemental Figures Legends

Supplemental Figure 1. Identification of the 127D01 epitope. (A) Synthetic peptides corresponding to the full-length extracellular domain from CXCR2 or fragments were synthesized by solid-phase peptide synthesis using Fmoc protection of the peptide backbone and purified by reverse-phase HPLC. (B) Peptides were used in a competitive ELISA in which soluble peptides compete for binding with a conjugate consisting of GFP fused with CXCR2 ECD immobilized on the ELISA plate. (C) Representative data from a competition ELISA experiment. Data points represent mean \pm SD from duplicate experiments.

Supplemental Figure 2. Schematic representation of the constructs and confocal images in S2R+ cells. (A and B) Transcriptional elements promoter and SV40 of the expression vectors, the different protein coding modules are represented as colored filled boxes. (C and D) Individual transfection results of VHH05 and 127D01 vectors in S2R+ cells. Confocal images show the distribution of fluorescent proteins in the cell. (E) Confocal images of co-transfection of NbVHH05-GFP with different cell compartments mCherry-VHH05 vectors showed the co-localization signal of GFP and mCherry. (F) Confocal images of co-transfection of Nb127D01-GFP with different cell compartments. mCherry-127D01 vectors showed the co-localization signal of GFP and mCherry. (G) Vectors information of NbVHH05-mCherry and mito-GFP-VHH05. Confocal images of co-transfection of these two vectors showed the co-localization signal of GFP and mCherry. (H) Vector information of Nb127D01-mCherry and mito-GFP-127D01. Confocal images of co-transfection of these two vectors showed the co-localization signal of GFP and mCherry.

Supplemental Figure 3. Different types of purified NbVHH05 and Nb127D01 and immunofluorescence examples. (A) Direct labeling can be achieved by linking purified nanobodies with different fluorophores indirectly by antibody labeling or site-specifically by sortase-mediated labeling. (A1) Schematics of NbVHH05 and Nb127D01 with fluorophore-488, 555 or 647. (A2) Confocal images showing direct immunofluorescence with NbVHH05-555 and Nb127D01-647 in S2R+ cells. (A3) Confocal images showing direct immunofluorescence with NbVHH05-555 prepared by sortase-mediated labeling. (B) Schematics of indirect labeling with nanobodies containing ALFA-tag, HA-tag, biotin or human IgG as primary antibodies and confocal

images in S2R+ cells.. (B1) NbVHH05 and Nb127D01 detected with anti-VHH IgG antibody. (B2) NbVHH05 and Nb127D01 with ALFA-tag detected by NbALFA. (B3) NbVHH05 and Nb127D01 with HA-tag detected by anti-HA antibody. (B4) NbVHH05 and Nb127D01 with biotin prepared by sortase-mediated labeling detected by streptavidin. (B5) NbVHH05 and Nb127D01 with Human IgG detected by anti- Human IgG antibody. Bar: 10 um.

Supplemental Figure 4. Nanobodies purification and fluor-conjugation. (A and B) Coomassie brilliant blue staining of ALFA- and HA-tagged nanobodies using *E. coli* protein expression. (C) Fluorescence signals results of fluor-conjugated nanobodies under 555 and 647 channels.

Supplemental Figure 5. Test of potential interaction between VHH05 and 127D01.

(A) Fluorescence confocal results showed no co-localization signal. Co-transfection of Nb127D01-GFP and mito-mCherry-VHH05 or H2B-mCherry-VHH05, NbVHH05-GFP and mito-mCherry-127D01 or H2B-mCherry-127D01 in S2R+ cells. (B) Western blots indicate no cross interaction between the two systems. Lysates from S2R+ cells transfected with different types tagged vectors (as in Figure 1) or a mock control plasmid were analyzed by SDS-PAGE and western blotting. The blot was developed with NbVHH05-ALFA and Nb127D01-ALFA, followed by NbALFA-HRP or a mouse anti-tubulin primary antibody, and followed by anti-Mouse IgG HRP.

Supplemental Figure 6. Test of nanobodies concentration gradient. Lysates from S2R+ cells transfected with H2B-mCherry-VHH05 or H2B-mCherry-127D01 were analyzed by SDS-PAGE and western blotting. The blot was developed with NbVHH05-ALFA and Nb127D01-ALFA with a concentration gradient from 1:100, 1:1000, 1:10000, 1:100000, followed by NbALFA-HRP or a mouse anti-tubulin primary antibody followed by anti-Mouse IgG HRP. Two conditions of long-time exposure (60 s) and short time exposure (20 s) were set for signal reading.

Supplemental Figure 7. Rapid production of nanobodies in S2 cells for western.

(A) Workflow production of nanobodies in the fly cell line. (B) Western blot using culture media containing Nb127D01-hIgG, detected by anti-hIgG-HRP. (C) Western blot using culture media containing NbVHH05-hIgG, detected by anti-hIgG-HRP. Five different concentrations and three exposure times were used.

Supplemental Figure 8. Transgenic vectors information and test in S2R+ cells.

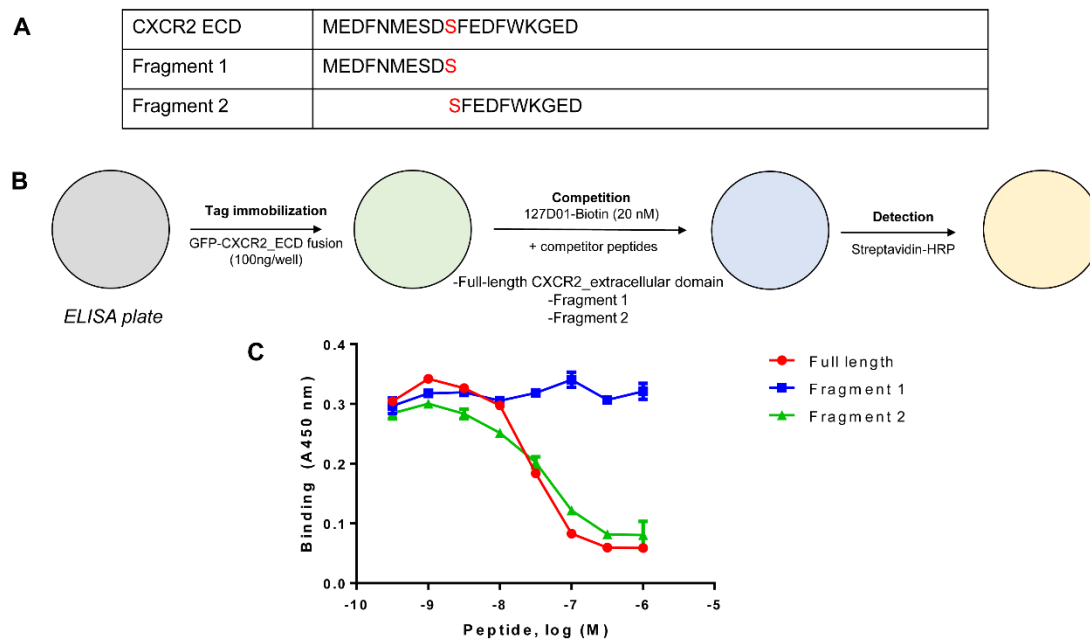
(A) Series of UAS vectors expressing NbVHH05 and Nb127D01 fused to GFP and HA or containing BiP signal. Transcriptional elements promoter and SV40 of the expression vectors, the different protein coding modules are represented as colored filled boxes. (B) Lysates or culture media from S2R+ cells transfected with GFP vectors were analyzed by SDS-PAGE and by western blot. The blot was developed with anti-GFP antibody or anti-tubulin antibody. (C) Lysates or culture media from S2R+ cells transfected with HA vectors were analyzed by SDS-PAGE and by western blot. The blot was developed with anti-HA antibody or anti-tubulin antibody. (D) Two

types of UAS vectors for overexpressing NanoTag labeled genes. N-, C-terminal of POI contains VHH05 and 127D01. BiP is the signal for labeling secreted proteins. (E) Five secreted proteins and three cytoplasm proteins were labeled, and their sizes are indicated. (F) Western blot results of three small size secreted proteins, Akh and Dilp8 showed multiple bands, and Dilp2 only showed a single band. (G) Western blot results of Pvf1, Upd2, REPTOR-bp-B, REPTOR-bp-C, REPTOR-bp-B. The blot was developed with NbVHH05-ALFA and Nb127D01-ALFA followed by NbALFA-HRP in F and G.

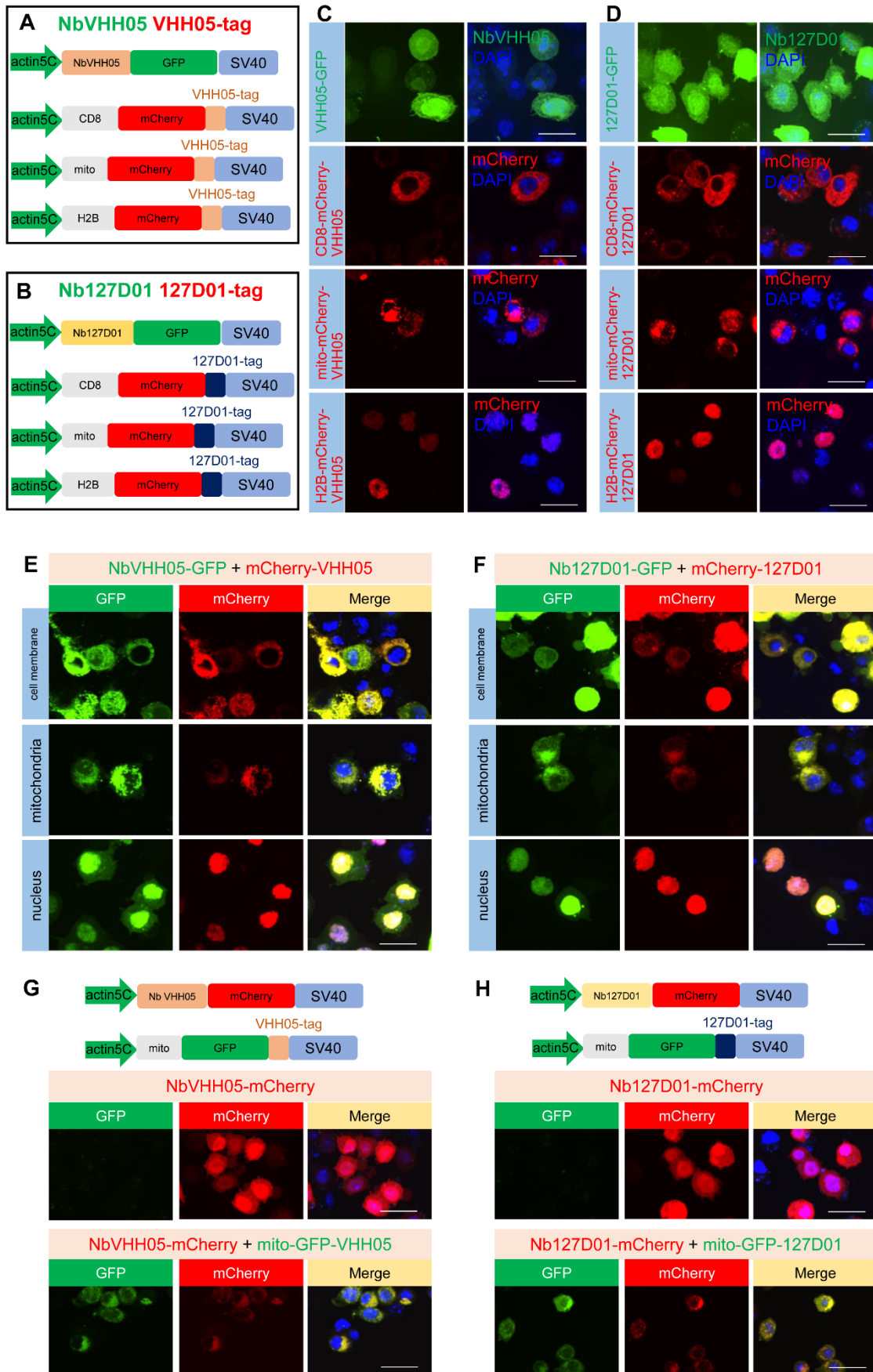
Supplemental Figure 9. Schematic representation of the CRISPR/Cas9-mediated gene KI approach and the targeted integration of transgene constructs. (A) Schematic representation of the *H2Av* gene and the sgRNA targeting site. The thin gray line represents the *H2Av* genomic locus, with open boxes indicating the promoter, exons, and poly(A) signal. A 164-bp fragment (gray box) located at the 5' end represents the 5' UTR. The two 79-bp, 119-bp and 233-bp fragments (pink boxes) are exon 1, exon 2 and exon 3, respectively. A 322-bp fragment (gray box) located at the 3' end is the poly(A) signal. The red lightning icon indicates the sgRNA site. In the PHD donor construct, the DsRed2 marker expression cassette is driven by the eye specific 3xP3 promoter. DNA fragments of 999 bp and 999 bp at the 5' and 3' ends were PCR-amplified, subcloned into vectors, and used as homology arms (5' HR and 3' HR, respectively). The 3xtag sequence is shown in the green box. 3' terminal repeat and 5' terminal repeats are the piggyBac transposase recognition sequences. Primer positions for amplification analysis of the integrated insertions in transformed flies are shown by arrows. Primer pairs of F1/R1 and F2/R2 were used to amplify the 5'- and 3'-end insertion junctions, respectively. The donor plasmid and sgRNA were injected into the embryos and the donors integrated into the genome. Positive individuals were screened for red fluorescence of the eye. The selection marker was removed by crossing with flies expressing the transposase. Primer pairs of F3/R3 were used to amplify the final insertion. (B) PCR amplification was used to confirm the insertions. Two *H2Av-3x127D01*, four *H2Av-3xVHH05* heterozygous and *w1118* genome DNA were used as template and the thick gel bands showed the corrected insertion. (C) Sequencing results of the integrated diagnostic DNA fragments showing 3xtag genome–donor integration.

Supplemental Figure 10. Indirect or direct immunostaining of *H2Av-3xVHH05* flies. (A and B) Adult female guts were dissected and stained with NbVHH05-biotin and visualized by Streptavidin-488. (C and D) Adult female guts were dissected and stained with NbVHH05-555. A and C were *w1118*, B and D are *H2Av-3xVHH05*.

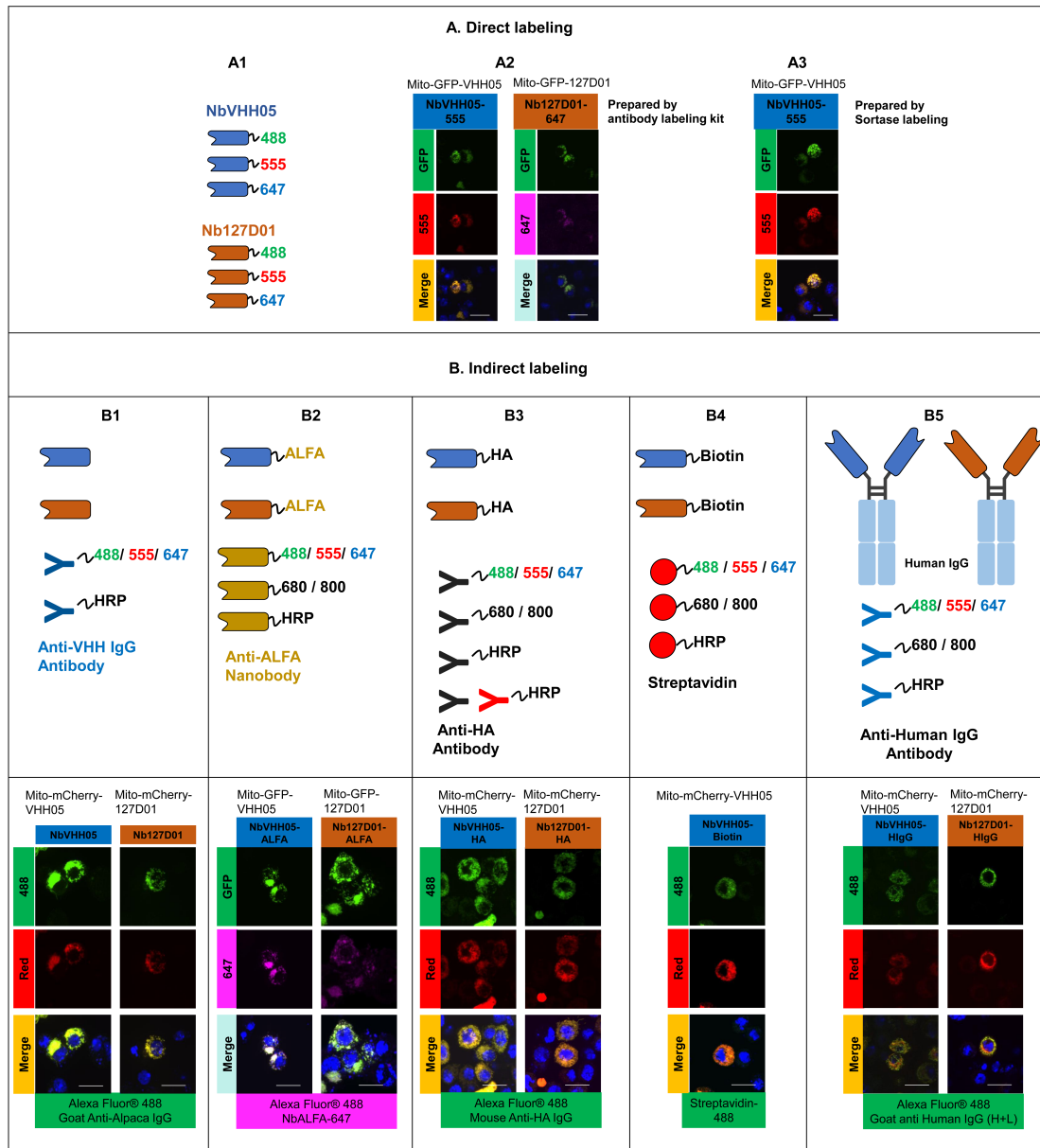
Supplemental Figure 1



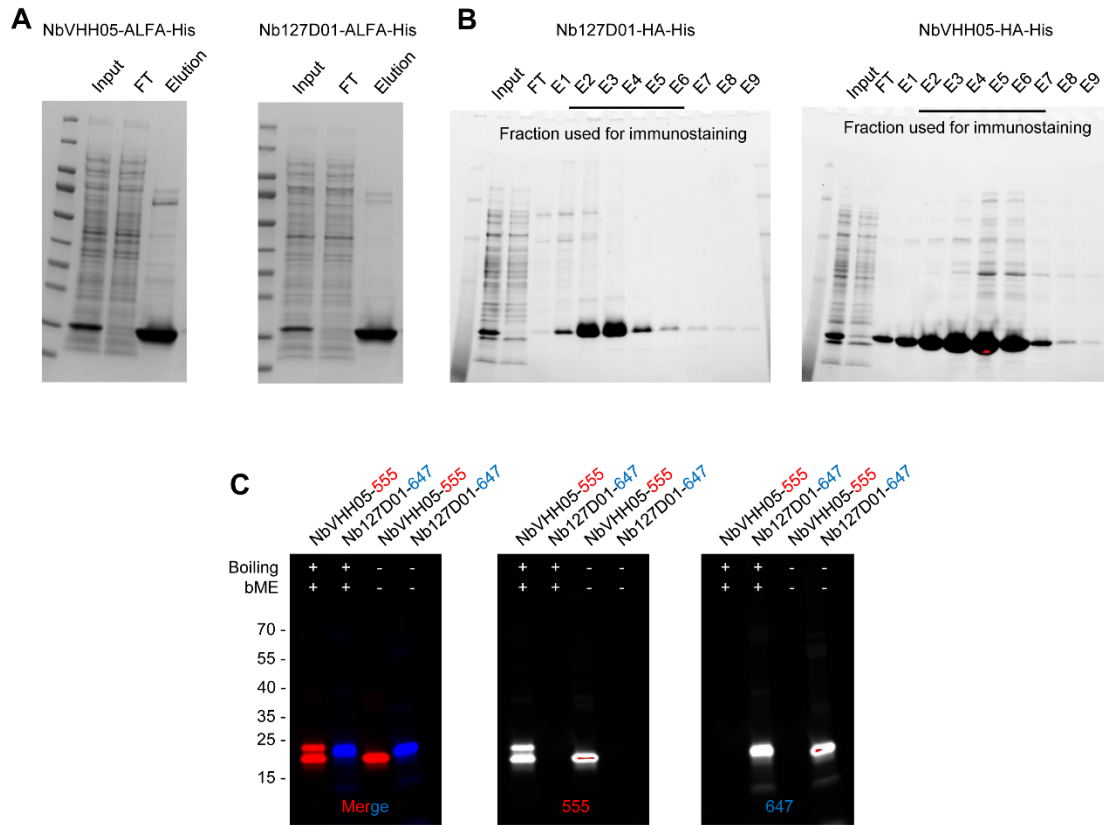
Supplemental Figure 2



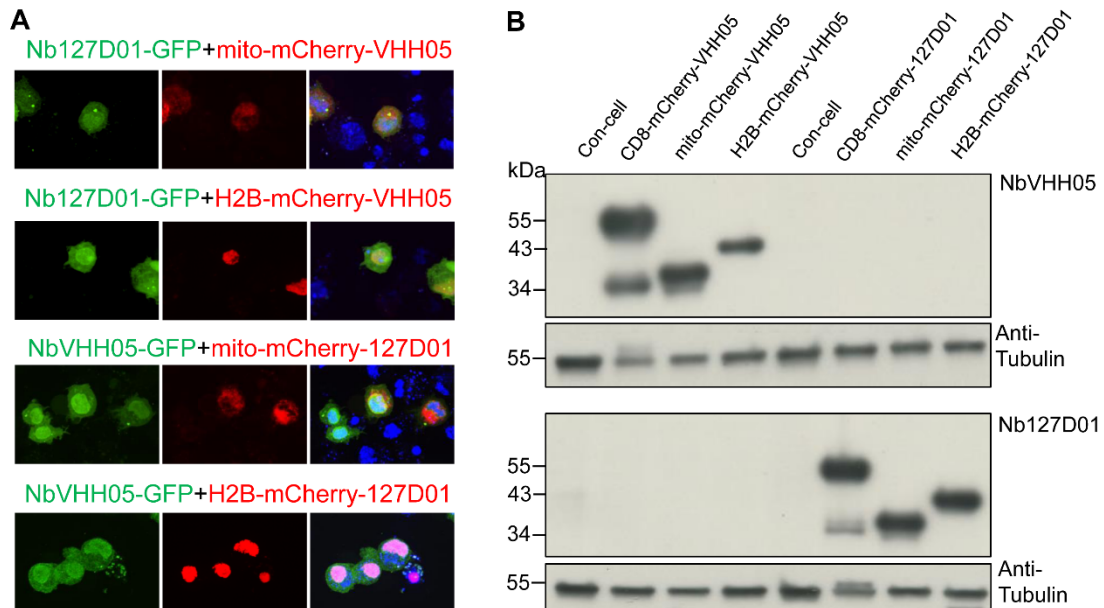
Supplemental Figure 3



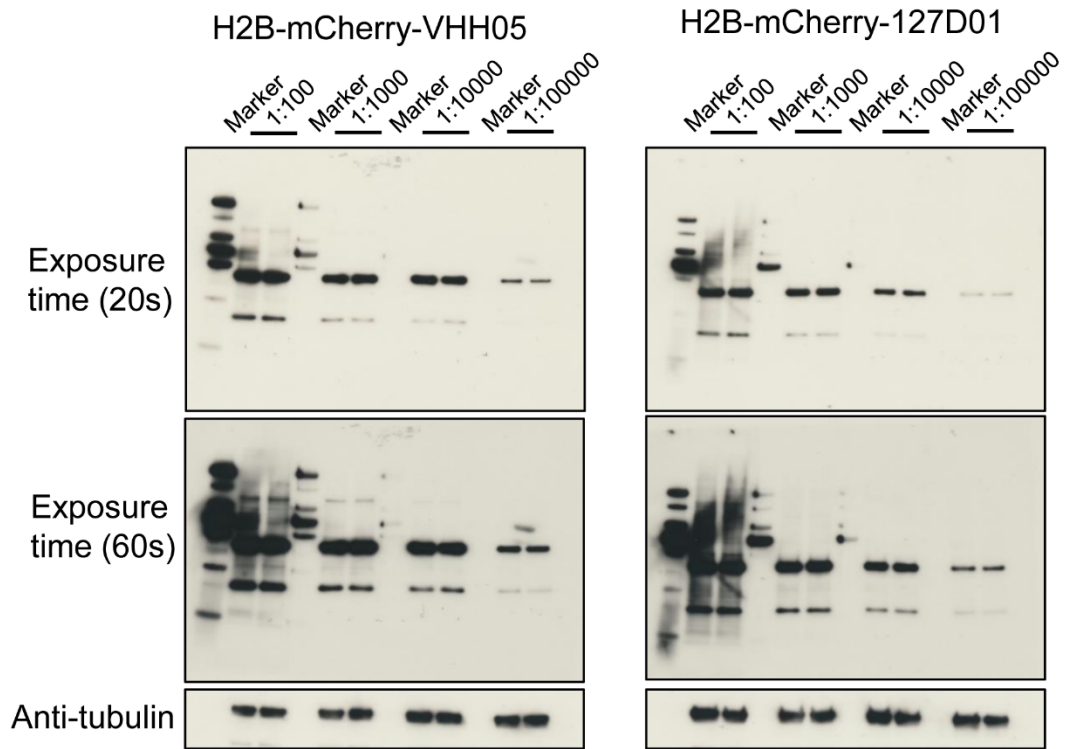
Supplemental Figure 4



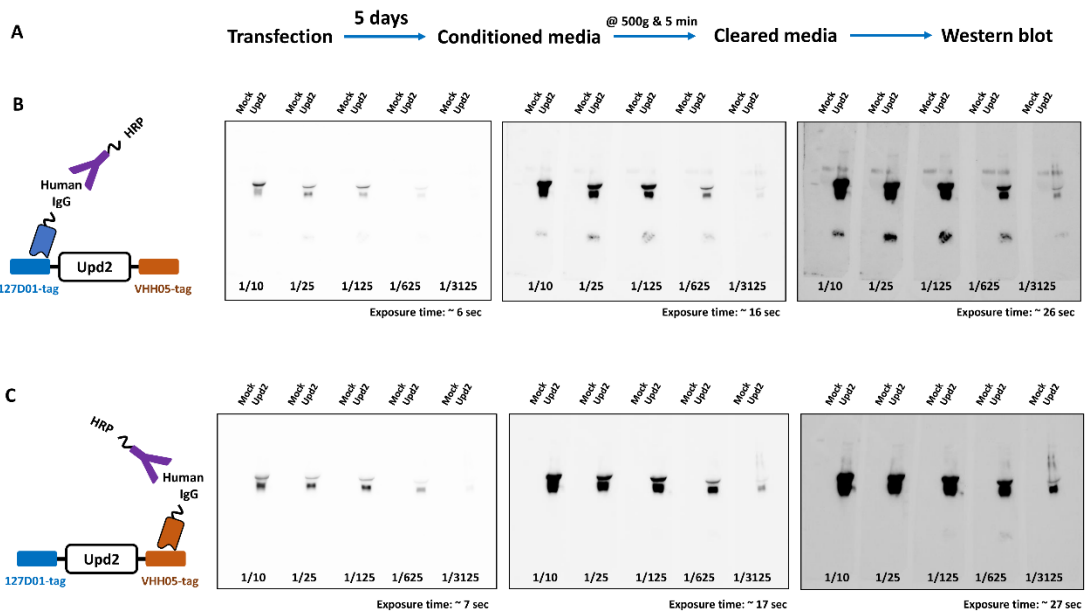
Supplemental Figure 5



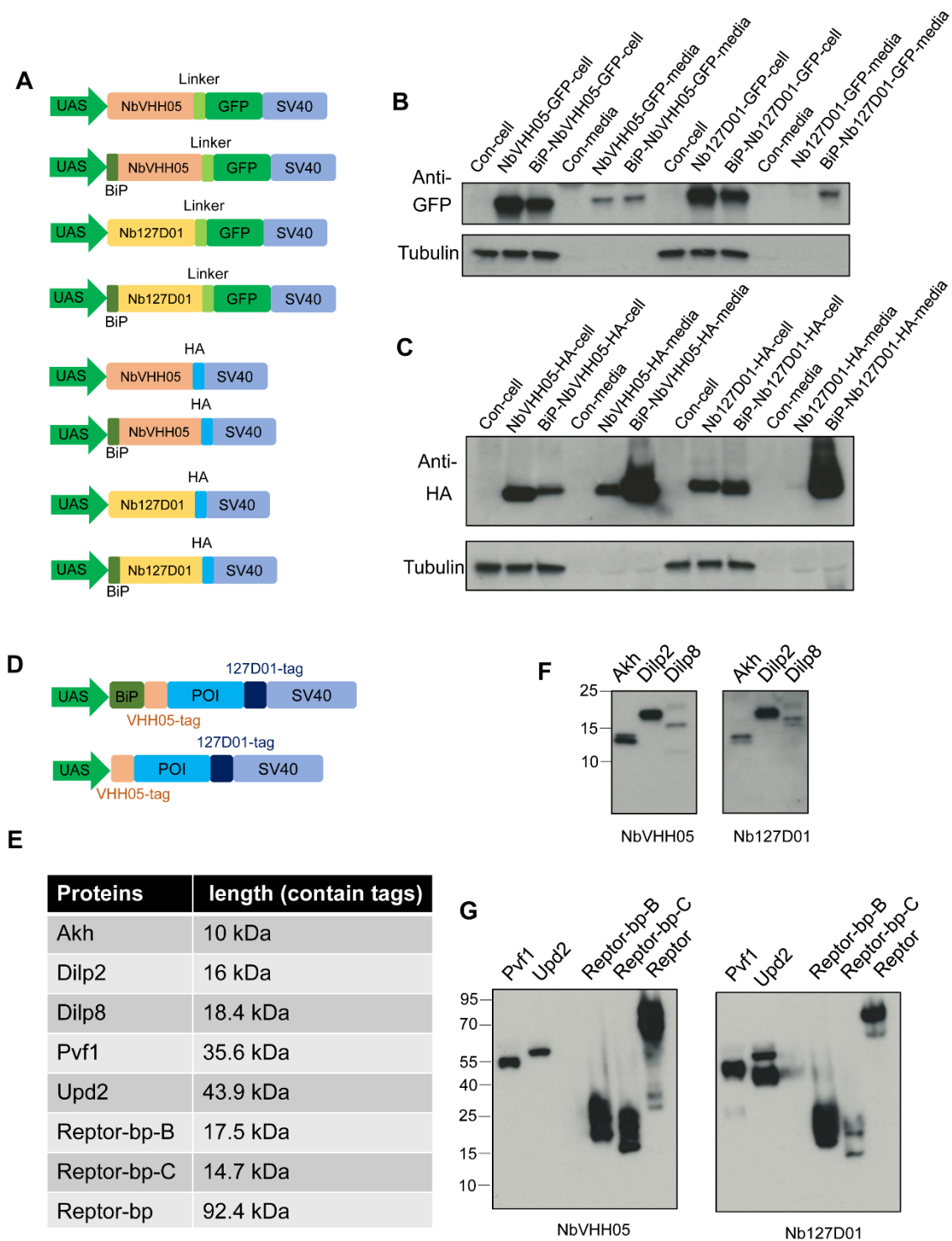
Supplemental Figure 6



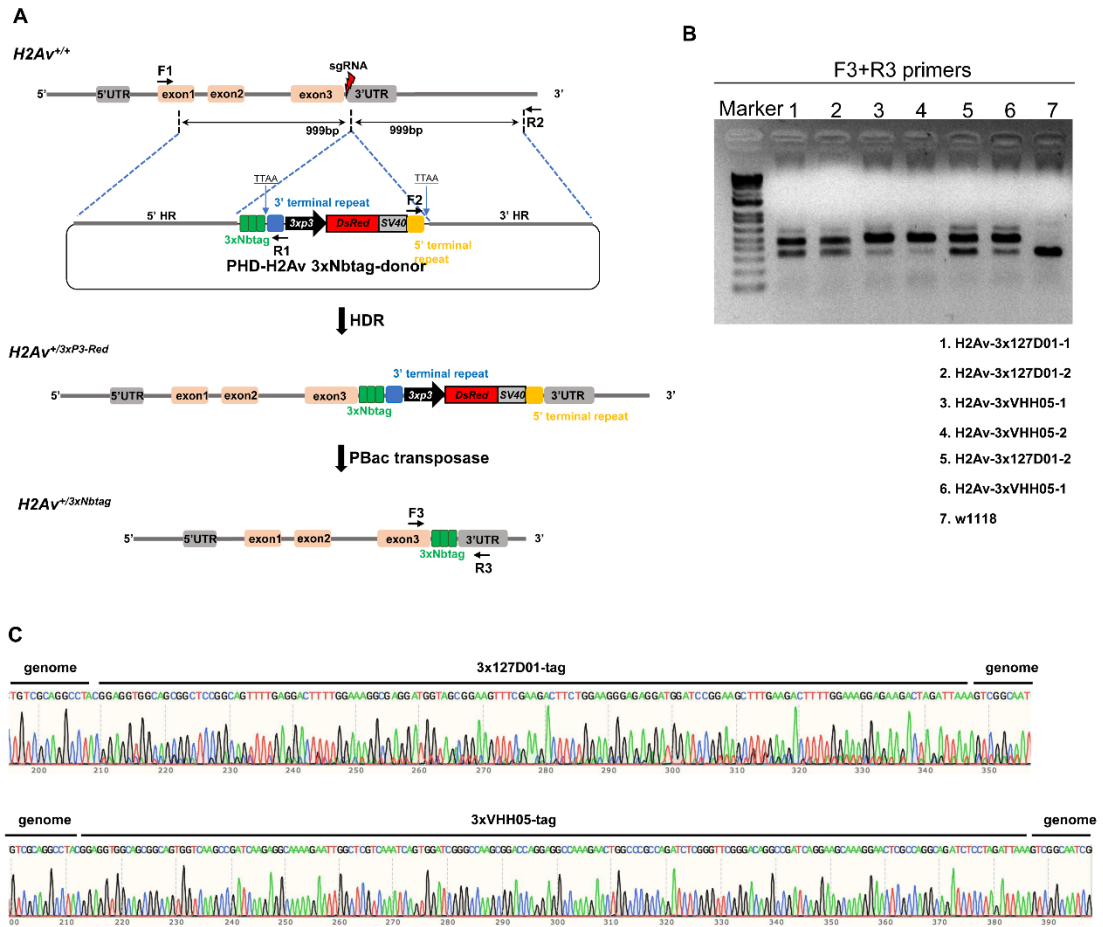
Supplemental Figure 7



Supplemental Figure 8



Supplemental Figure 9



Supplemental Figure 10

